CONFIDENTIAL

Improved control of an IV administration system

Design of a sensing and regulating method to improve the control of gravity based intravenous (IV) therapy

M.B. Disselkoen

Master of Science Thesis

TU Delft

MSCCONFIDENTIAL

Improved control of an IV administration system

Design of a sensing and regulating method to improve the control of gravity based intravenous (IV) therapy

Master of Science Thesis

For the degree of Master of Science in Biomedical Electronics at Delft University of Technology

M.B. Disselkoen

January 19, 2017

Faculty of Mechanical, Maritime and Materials Engineering (3mE) · Delft University of Technology

The work in this thesis was supported by NXP. Their cooperation is hereby gratefully acknowledged.

Delft University of Technology
Department of
Biomedical Engineering

The undersigned hereby certify that they have read and recommend to the Faculty of Mechanical, Maritime and Materials Engineering (3mE) for acceptance a thesis entitled

Improved control of an IV administration system

by

M.B. Disselkoen

in partial fulfillment of the requirements for the degree of

Master of Science Biomedical Electronics

Dated: January 19, 2017

Supervisor(s):

prof.dr.ir. P.J. French

dr.ir. A. Nackaerts (NXP)

Reader(s):

dr.ir. J.F.L. Goosen

dr.ir. F. Sebastiano

Abstract

Intravenous therapy is the most common way for the delivery of substances to (hospitalized) patients. The amount of patients receiving some form of Intravenous (IV) therapy is enormous ($85-90\%$). Different techniques exist for the administration of IV fluids. The two main administration techniques are: active (pump based) and passive (gravity based). The active devices are expensive, self-regulating and deliver fluids at a high accuracy. The passive devices are low priced, manually controlled (requiring periodic re-adjustment), and are not accurate. Improvement of the administration control of these passive devices can reduce the cost of therapy, improve the quality of care and make high quality IV therapy more widely available. Current passive devices are configured by the caregiver that manually sets a flow adjusting tube clamping device, based on the flow rate. The readout of the flow rate is performed by visually counting drops in a drip chamber integrated in the administration set. This method of regulation is time demanding and prone to error. Therefore, the main goal of this research project is the development of a sensing and flow regulating method, that improves the control of these passive IV administration devices.

A new technique for both flow rate sensing and flow rate adjustment are presented. The flow rate sensing technique makes use of a combination of two sensors. One sensor detects the drip rate by measuring the change of capacitance resulting from the drop formation. The second sensor detects the reservoir fluid level by measuring the change of pressure inside the drip chamber. This combination of sensors facilitates accurate overall flow rate sensing by combining short and long term flow rate information. The rate of flow is regulated by a designed magnetically linked needle valve. The magnetic link facilitates the external control by a servo, of a plunger assembly inside the drip chamber, without breaching the sterile IV flow. The plunger adjusts the rate of flow by restricting the outlet of the drip chamber. A routine for an IV controller is presented, that makes use of the combined sensor actuator system. The reservoir fluid level information is used in the routine as feedback for the estimation of the drop volume of the detected drops.

The new sensor and actuator system was tested in a test setup controlled by a single Integrated Circuit (IC). The measurements of the two sensors showed the variation of flow rate created by the actuator. To conclude, based on the performed tests the developed sensing and regulating method seems promising for the control of IV administration. However, further research and optimization is required for the implementation of the actuator and sensors in a self-regulating IV administration system.

Table of Contents

Preface

Coming from a mechanical engineering bachelors, NXP Leuven is not the most logical place to do your master thesis. This project however combines some biomedical, electrical and mechanical engineering. A great combination that matches really well with my field of interest. Prof. Paddy French understood this the moment I entered his living room located at the TU Delft. Moving to Belgium was an interesting experience and luckily some of the younger guys at NXP taught me how to blend in, although I would of course always be "den Hollander". Or maybe for some: the strange "Hollander" repairing his broken Citroën BX in the parking lot. The contrast between development boards, test equipment, endless random other electronics and the IV setup in my room, triggered some interesting conversations at NXP.

The weekly meetings and the brainstorm sessions with Axel Nackaerts, my supervisor at NXP were great. His fast analysis and electronic approach to mechanical problems were really interesting. Thank you for supervising me during this project and making it possible to file two patents: I could not have imagined that I would finish my thesis as an official inventor! I would also like to thank Paddy French for advising me to contact NXP Leuven in the first place and for his guidance and feedback during this project. Furthermore I would like to thank Hans Goosen and Fabio Sebastiano for reading my thesis and taking part in the final stage of my graduation process.

Finally I would like to thank my family and girlfriend for their endless support and motivation during this project, but even more during the rest of my education. I am looking forward to present and defend my master thesis project during the public presentation on January 19th 2017.

Micha Disselkoen
Den Haag, January 9, 2017

Chapter 1

General introduction

In this chapter a general introduction will be given into the background of the conducted engineering research, the definition of the research question and the ways the research question will be answered.

1-1 Background

1-1-1 What is IV Therapy?

Various medical treatments require the delivery of substances into the human body. When the delivery takes place into the cardiovascular system, rapid distribution of the substance is accomplished. Intravenous (IV) therapy is a way of delivering a substance directly into the circulatory system via a vein. IV therapy denotes the method by which these substances are injected, as the actual treatment depends on the type of substance injected. Typical substances that are delivered intravenously are:

- fluids [1]
- blood
- drugs
- electrolytes

Because of the efficiency of the therapy, IV has become the most common route for the delivery of these substances to (hospitalized) patients. With around $85 - 90\%$ [1][2] of hospitalized patients receiving some form of IV therapy in the western world, the amount of users is enormous.

[1] all substances are injected in the form of fluids but with "fluids" the injection of fluid-replacement liquids is meant (e.g. saline solution)

A typical setup for IV therapy consists out of three main components: the reservoir, an (active) flow regulating device and a tubing/venepuncture device. The type of substance injected determines the components that can be used. For example, the injection of certain drugs require a more precise (low) flow delivery, while hydrating fluids can be injected with higher flow margins. These requirements lead to different working principle for the flow regulating device. Two groups of devices can be distinguished:

1. Passive (gravity based)
2. Active (pump based)

The passive (gravity based) devices use the hydrostatic pressure gradient created by an elevated reservoir to initiate the flow of a substance from the reservoir through the catheter into a vein. The flow is regulated by increasing or decreasing the tubing resistance with a clamp. The active (pump based) devices use the principle of motorized displacement of fluid. Flow regulation is accomplished by adjusting the rate at which the fluid is actively displaced.

1-1-2 Variation of use cases

As IV therapy is such a broadly applicable treatment, it is used in many different situations. Each use case has specific requirements for the IV setup. As an example three typical situations/locations are:

1. In the third world/developing countries the hygienic standards are low. This results in frequent epidemics of diarrhoea. One of the life threatening effects of diarrhoea is dehydration, which is typically treated by the supply of fluids via IV therapy. During an epidemic of diarrhoea many patients need to be treated with a minimum of nurses. This situation requires cheap, simple, robust and quickly configurable self-regulating IV administration sets. If the system is simple to configure and self-regulating, nurses will be able to use time more efficiently, thereby increasing the total amount of patients that can be treated.

2. In western hospitals increase of efficiency and improvement of the quality of care is a continuous goal. Most (90% [1][2]) patients in a hospital continuously receive IV therapy with fluids. This stable stream of fluid is a transport medium that can be used to carry drugs. Accurate supply of the steady fluid stream is controlled by a flow regulator configured and checked by the nurse. Stability improvements of the regulator reduce the need for periodic checks of the IV system by the nurse, resulting in more efficient time allocation for the nurse and potentially also improving the quality of care.

3. Emergency situations are often chaotic and can occur at any location. Distraction from critical tasks that require attention of the doctor should be minimized. An ideal IV system in such a situation would be mobile, self-regulating, battery powered and quickly and easily configured.

1-1-3 Limiting factors of (improving) IV therapy

The aim of gradually supplying a substance into the circulatory system is to maintain a certain concentration of the substance in the body. Ideally the system measures the concentration in the body and regulates accordingly. When this is not possible, a certain infusion rate is assumed to result in the aimed treatment. For every type of substance a patient specific flow rate and margin is therefore defined. When an anomaly occurs under- or over infusion can be the result, leading to potentially dangerous situations for the patient. The technique of IV therapy is among the most frequently occurring technology-related sources of medical errors [3]. Inaccurate infusion flow is one of the reasons for this.

The type of technology used for IV therapy is a delicate balance between the cost, risk and quality of care. Low risk infusion flows with wide margins can be handled by low cost passive (disposable) administration sets (under 10 dollar), while high risk flows need to be handled by expensive (reusable) active systems costing between 1200 to 3500 dollar. This delicate balance even differs depending the use case (1-1-2), and location of use. While balancing between the different properties is not unique to IV technology, it's widespread use and related broad range of risk, cost and quality are. The sole physiological principle of IV therapy thereby requires many different technical solutions that suit specific use case needs. An improvement of the therapy can be accomplished by improving one or more of them.

1-2 Problem statement

When the different devices in use for IV therapy are laid out based on price and performance, a remarkable gap forms: devices are either really low priced, simple and low performing or accurate, complex and expensive. The main reason for this is the two different working principles of these devices: active and passive (1-1). The aim of this research is to reduce this gap by improving the low priced passive gravity flow devices. These improved low-end devices might then replace the expensive active devices in some medical situations, leading to better cost-effectiveness. To improve the existing gravity based low performing and difficult to regulate devices, new sensing and regulation methods are necessary. Leading to the research question:

> **What kind of sensing and regulating method can be used to improve the control of gravity based Intravenous (IV) therapy?**

1-3 Design strategy

The development of a more controllable technique for gravity based IV will be done by separating the system in three parts:

- Sensing
- Actuation/control
- Integration

Each of these answer part of the research question. The sensing part (chapter 3) will elaborate on the development of a new sensing technique for the system. Its final goal is a sensor method that delivers usable information to the controlling system. The actuation part (chapter 4) discusses a new technique for the regulation of flow in the system. The controllability can only improve when the combination of both sensor and actuation function together. This integration is discussed in the chapter 5.

Chapter 2

Intravenous therapy

The first step in the design process is to understand the way the existing system/therapy works, and identifying the critical parameters. In the introduction the principle of Intravenous (IV) therapy is explained. This chapter analyses the functioning principals of IV therapy and the essential elements.

2-1 IV therapy administration requirements

Typical IV therapy starts by a prescription of a doctor that made an assessment of the patient. The prescription together with technical and economical boundary conditions, forms the input for the decision for a specific IV administration technique. We first focus on the technical part of the therapy. In later stages of IV therapy improvements, all of these inputs should be taken into account. The technical requirements more specifically concern: flow, ergonomics (mobility, weight) and presence of safety mechanisms.
Dominant for the design of a sensing and regulating method are the flow requirements. Volumetric flow rate (Q) is defined as the volume of fluid (V) that passes per unit of time (t):

$$Q = \frac{V}{t} \tag{2-1}$$

In the case of IV therapy, flow requirements are specified over different timescales. The multiple flow requirements arise as for certain therapies, changing the flow rate within short periods of time is allowed as long as a predetermined flow is supplied over a longer timescale. Other therapies require more constant flow without significant interruptions. The type of IV therapy that is given (depending on the sort of fluid that is supplied), combined with patient specific conditions, forms the flow rate requirements.

The selection of a specific technique is done by comparing the performance of a device with a flow performance curve named the trumpet curve (Fig. 2-1). This trumpet curve presents

the flow rate error of a device over time relative to the aimed flow. The layout of the trumpet curve and the test method associated with it, are standardized to be able to compare the performance of different devices [4].

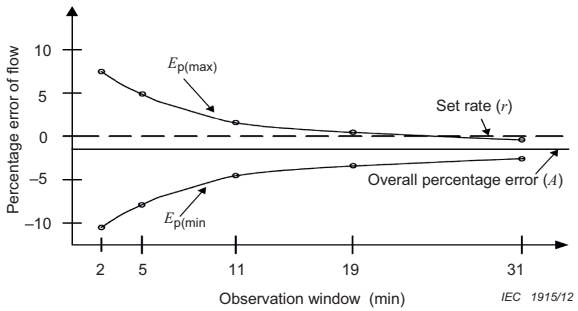

(a) Trumpet curve model, image source: [4]

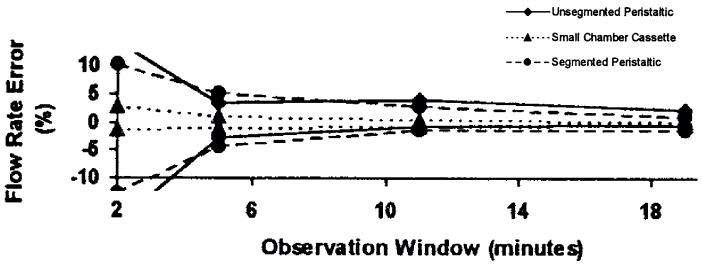

(b) Trumpet curve for several representative large volume infusion pumps operated at 5mL/hr, image source: [5]

Figure 2-1: Model of trumpet curve as described in IEC60601 and example of use with different pump systems

The overall flow performance of a device, thus poses a limit on the type of therapies that it can be used for (see critical performance parameters in appendix A). As a result, relatively low performing devices can be of use when they suit the needs of a certain form of IV therapy in a better way than existing devices do. The research question is aimed at finding a method for improving control of gravity based IV. The 'new' method should therefore, strictly from technical point of view, outperform the flow performance at any point compared to the performance of existing gravity based IV regulators. From the economical or practical point of view, reduction of price or increased usability, while keeping performance at an equal level, can be seen as an improvement.

2-2 Gravity based IV

The gravity based IV is the simplest technique in use for IV therapy. It is generally used for lower demanding types of IV therapy, where therapeutic range of supply is relatively wide, as for example fluid resuscitation. During gravity based IV, pressure follows from the height difference between patient and reservoir, and control over flow is accomplished by increasing or decreasing resistance in the tubing downward of the reservoir. The technique can only be used with venous infusion therapy and not with arterial infusion as arterial pressure is higher than the hydrostatic pressure generated by the elevated reservoir.
The device used for IV therapy is the so-called administration set. The set consists out of multiple coupled parts and always contains a reservoir, a drip chamber, a flow regulating device, tubing, a connection port, and a catheter [6] (see Fig. 2-3) . One of the essential parts for flow rate control is the drip chamber. It has two functions: firstly, it degases the fluid, and secondly it forms the drops. These drops are used by the caregiver to get an indication of the flow rate. A certain amount of drops in a defined time window equals a rate of flow.

As drops are used as an entity of a certain volume, defined drops need to be created. The size of these drops is defined in the amount of drops that equal one millilitre. Generally two main sizes of drop formation are used: macro and micro drop, corresponding to respectively 20 and 60 drops per millilitre.
Therapy is setup by the caregiver, by calculating the amount of drops that should drip in a certain time to reach the prescribed flow rate and by setting the flow regulating device (generally a roller clamp) to adjust the dripping rate until it complies with the prescription. As therapy progresses regular check-ups and readjustment of the flow rate are necessary. Flow variation is caused by a gradually lowered water head level of the reservoir on the long term, and a changing venous pressure on the short term [7].

2-3 Intravenous fluid supply model

In essence, IV fluid administration is a flow initiated by gravity or pump from a reservoir through tubing into the internal 'tubing' (circulatory system) of the body. Either the pump or the height difference of the reservoir provides the pressure for flow through the system. Every part thereafter functions as a resistance and results in a pressure drop. Insight into the pressure drop resulting from tubing (and cannula) of the system can be gained by using the Hagen-Poiseuille's equation for laminar flow in a straight tube:

$$Q = \frac{\Delta p \cdot r^4 \cdot \pi}{8\eta \cdot L} \tag{2-2}$$

where:

Q = flow
Δp = pressure difference between exit and inlet of tube
r = radius of tube
L = length of tube
η = dynamic viscosity of fluid

It can be seen that in a steady laminar flow condition the pressure drop relates to the tube length and viscosity and inversely with tubing/cannula radius. This laminar flow condition (and the straight tube) is however not true for every instance and type of administration set. Modelling the therapy as a system with an initial pressure that's being reduced (as a result of pressure drop) by parts of the IV administration set and the circulatory system, does however give a great insight into the workings of the IV therapy principle. Such a model for the situation of gravity based IV is shown in Fig. 2-2.

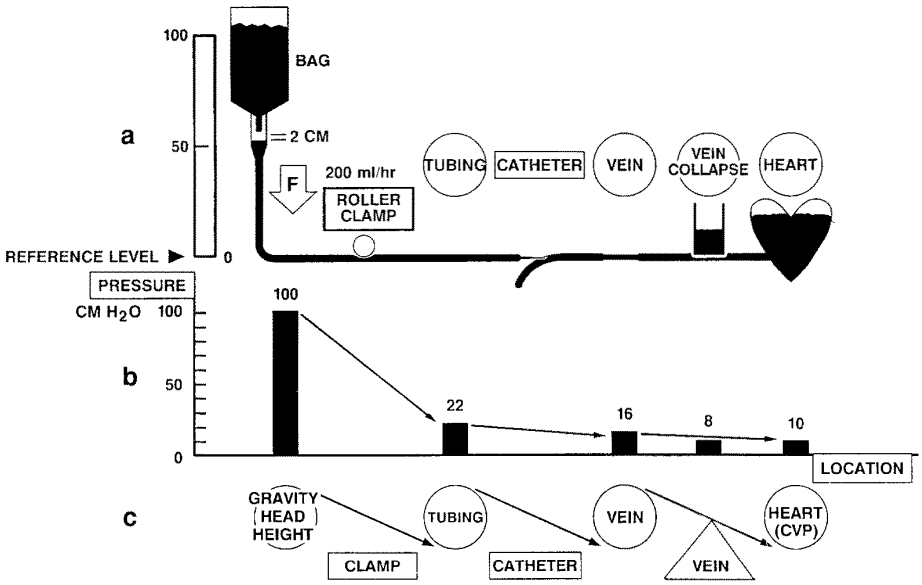

Figure 2-2: Model for manually controlled intravenous administration system and patient, image source: [8]

The pressure source is the IV bag. The resulting system pressure originates from the difference of height between fluid head in the reservoir, and the patient ($p = \Delta h \cdot \rho \cdot g$, generally around 60-100 cm above the right atrium of the patient [5]). The first resistance marked (the roller clamp) is a variable resistance that is used to control the rate of flow through the system. Further downstream, the pressure is reduced by tubing and the catheter. The catheter is the last component of the administration set before flow is injected into the circulatory system. A flow into the vein is only accomplished when the resting pressure at catheter tip exceeds the pressure that is required to open the vein (KVO pressure) and a possible back pressure (venous pressure) present in the vein. This is because veins can collapse completely if the internal pressure is low compared to pressure outside of the vein (comparable to a Starling Resistor). When the KVO pressure is reached, relative low resistance (and thereby pressure drop) results from the veins. The venous pressure and the height between patient and reservoir can change over time, resulting in changing rate of flow.
A similar model can be made for a setup with an IV pump, except for the fact that a pump delivers a certain flow independent of back pressure. It can therefore be seen as a flow source instead of a pressure source.

2-3-1 Functional parts

In figure 2-3, the essential parts of a gravity based administration set are displayed. Performance and dimensioning of the parts in this set are normalized by the 'ISO 8536-4'. In depth reviewing the flow regulating parts facilitates development of new methods of control. The following paragraphs will therefore describe the typical way these part function and their typical properties.

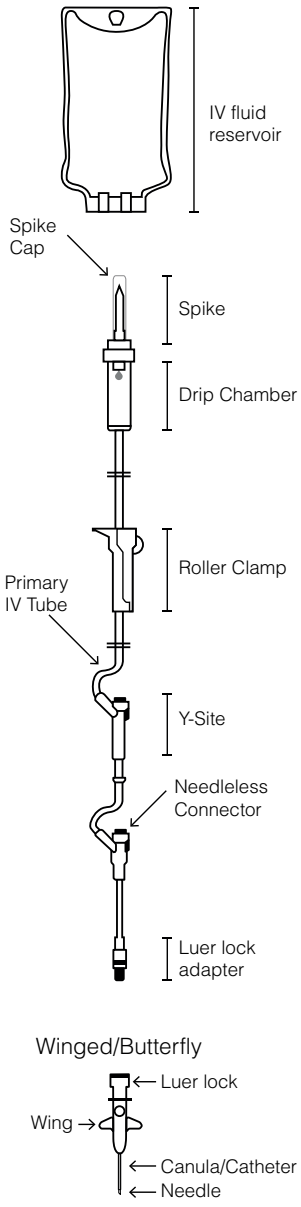

Figure 2-3: Components of a typical IV administration set

Reservoir

The IV fluid reservoir's function is to maintain the IV fluid and serve as a fixation point of the administration set to the IV pole (not displayed). One or two ports at the bottom of the reservoir serve as entrance/exit port. These can be used for the connection of the set or for injection of drugs with needles. The ports are typically kept shut with a flexible material that can be punctured by a needle and restores it shape and closing function after removal of the puncturing device. Three main types of reservoir exist, namely: soft, rigid and semi rigid reservoirs. The soft reservoirs are of the IV bag type. During emptying these bags collapses under atmospheric pressure. The rigid reservoirs can be made out of glass or another non-deformable material. These reservoirs cannot collapse and therefore need some form of venting to facilitate flow. The semi rigid reservoirs are deformable and deform during flow but still need venting for depletion.

Drip chamber

The rate of volume flow is measured by counting drops. These drops are formed in the drip chamber (see Fig. 2-5). The spike of the drip chamber pierces one of the ports of the reservoir. A small opening in the spike (2a) creates the fluid path from reservoir to drop forming orifice (2b). During setup of therapy the caregiver squeezes the soft part (4) of the drip chamber. Air is pushed out of the chamber into the reservoir until about $^1/_3$ of the reservoir is filled with fluid. The other part of the reservoir (3) is functioning as an air bubble, trapped inside the fluid path. This air bubble gives space to the formation of drops and facilitates degassing of the liquid.
At the bottom of the chamber (5) a fine gauze, filters outgoing IV fluid. This filter also prevents the administration set from emptying completely, thereby risking the injection of air into circulatory system of the patient.

Vented or non-vented When rigid or semi rigid reservoirs are used, venting is required. This is accomplished by the inlet from 1a to 1b. A small one way valve at 1a blocks fluid from flowing out of the reservoir, when the pressure inside the reservoir is lower than atmospheric pressure, air gets sucked into the reservoir via 1a. This air replaces the volume of the dispensed fluid.

Drop formation Drops are formed at the tip of the drop forming orifice. The orifice is fabricated in such a way (see Fig. 2-4a) that: "20 drops of distilled water or 60 drops of distilled water at (23±2) °C at a flow rate of (50±10) drops/min deliver a volume of (1±0,1) ml" [6]. Using the rate of drops as an indication of flow rate thereby has an inaccuracy of at least ±10%. During actual therapy multiple factors influence the size of the drop. Namely: the rate of flow, orifice size, orifice shape and fluid properties. The general relation between drip rate and drop size is that at lower rates the drop size decreases (see Fig. 2-4b), thereby increasing the amount of drops in one millilitre.

Tubing

Flexible transparent tubes are used to connect the different components of the set. Regulation with a roller clamp is accomplished by squeezing the tubing. The physical properties of the tubes makes it hard to reduce the flow to zero. When the tube is compressed between two flat surfaces, the material and design of the tube results in the formation of two smaller tubes (see Fig. 2-8).

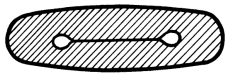

Figure 2-8: Squeezed IV tube forming two separate channels, image source: [7]

Roller clamp/Regulation

The roller clamp/regulation device facilitates regulation of infusion flow between zero and the maximum. The simplest form of regulation is accomplished by compressing the tube just below the drip chamber. These devices are manually controlled and consist out of a roller that can slide through a contour path (see Fig. 2-7). Repositioning of the roller on the path results in compression of the tube by the roller. The tube is compressed between the roller and a profile that ensures the complete compression of the tube (see Fig. 2-6), compensating for the effect described in the tubing paragraph.

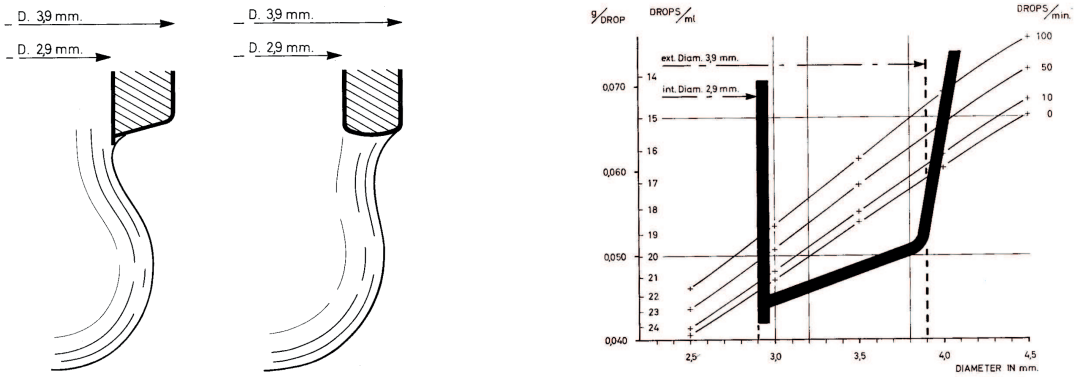

(a) Influence of orifice shape on drop size

(b) Relationship between drop size, orifice size and flow rate

Figure 2-4: Orifice shape and flow speed influence on drop size, image source: [9]

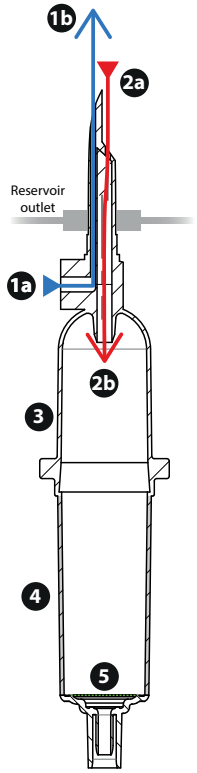

Figure 2-5: Section view of BBraun Intrafix® drip chamber. With vented air flow in blue and IV fluid flow in red.

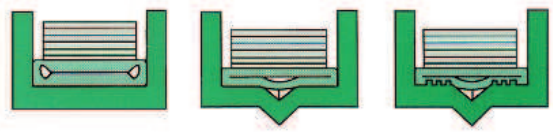

Figure 2-6: Clamping profiles of different roller clamps, image source: [10]

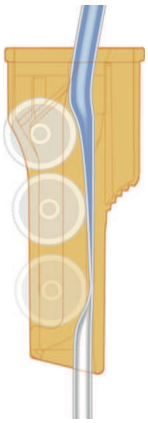

Figure 2-7: Section view of roller clamp with roller in multiple positions (image from: BBraun)

2-4 Complications of gravity based IV and the ideal system

The simplicity of the standard gravity based administration set has some drawbacks that lead to low performance. Apart from the gravity based working principle a lack of control is one of the main reasons for this low performance. The caregiver configures the system at a certain drip rate and after this initial setting no active feedback control is present. It is thus only correctly configured for the initial state of the system. During use multiple (external) factors influence the system, resulting in a deviation of flow rate over time. The caregiver has to periodically check the drip rate and adjust the roller clamp to match the prescribed flow rate. Periodic check-ups are also necessary as no feedback is given by the system about anomalies, like tube kinking or other blockages.

One of the main external influencing factors is the venous pressure of the patient [7]. The pressure difference, originated from the elevated reservoir, present between the tip of the needle and the vein, reduces if venous pressure rises (see Fig. 2-2), resulting in a reduced flow. This effect is not corrected by the initial setting of the roller clamp as its resistance remains (approximately) constant. The same effect exist in the situation for repositioning of the patient: when a patient elevates his or her arm with the IV injection site, injection pressure reduces as a result of decreased reservoir head 'level' (see section 2-3).

On top of these external factors, multiple properties of the administration set itself influence the performance of the system. The first component in line that influences the accuracy of flow, is the reservoir. A non-vented reservoir (typically a bag) deforms under atmospheric pressure during emptying. The material properties of the bag influence the resistance against this deformation. The relation between flow rate and deformation is such that flow rate reduces when the resistance of the material against deformation increases. The second influencing factor inline is the drip chamber. The size of the drop depends on the flow rate, fluid type and orifice shape/size. As the drops are used for the measurement of flow rate, an inaccuracy in drop size results in an inaccuracy of configured flow rate. The accuracy by which the caregiver is able to set the rate of flow relies on the volume accuracy of these drops. The last main influencing item is the roller clamp. The plastic material of the tube is

being stressed by the roller clamp. This mechanical stress results in creep (or cold flow) of the tubing material. The tubing material thereby slowly deforms at the pinching location of the roller clamp resulting in a change of flow rate over time.

The ideal gravity based IV system The aim of IV therapy is to maintain a predetermined concentration of a substance in the body to achieve a certain therapeutic objective. The ideal IV system would therefore measure the concentration of this substance and regulate the injection flow to correct for any deviations of the concentration. The essential element missing in the existing gravity based system is the lack of periodic control and feedback.

Chapter 3

Sensors

3-1 Introduction

When looking for a sensor solution, identification of the high level information that is to be known is essential. These are the parameters that are independent of the way the therapy is executed and form the essential principle. With Intravenous (IV) therapy these parameters boil down to three main ones:

1. The volumetric flow rate (mL/h)
2. The volume transported (mL)
3. The type of substance/fluid

These are the parameters that are prescribed by the physician and should therefore be followed. The last parameter (type of substance/fluid) has an influence on the IV therapy system, but is itself not regulated by the system. The first two are to be regulated by the system and should somehow be measured.

In an ideal case, number one can be concluded from number two and vice versa: if we know the exact rate of flow at any moment in time we are able to calculate the supplied volume. This is however, only possible if we know the exact value of one or two at any moment. A small error in flow measurement will lead to an accumulated error in fluid volume.

There are two possible options:

1. measure either flow or volume at an (nearly) infinite rate and with minimal error
2. measure both parameters independently (within acceptable errors)

The first option requires highly accurate, fast (expensive) sensors and electronics and is therefore not the preferred option. The second option requires the development of two sensors that can perform the measurement of the separate parameters. By combining the short term flow rate measurement with the long term knowledge of the transported volume, a self-correcting sensor system might be possible. The following paragraphs describe the development and tests of these two sensors.

3-1-1 System state overview

The state of the system influences the information that is sensed by the sensors. It is therefore useful to define the different states. Typically the IV system can be described by three main states:

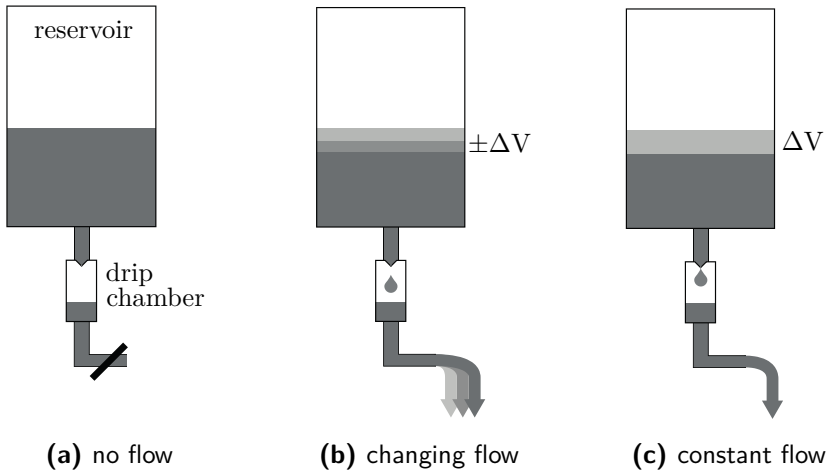

Figure 3-1: Model of main blocks IV setup. Three main states of the IV system are shown

In Fig. 3-1a the static no flow state is shown. The flow of liquid is blocked downstream of the drop forming location.

In Fig. 3-1b the system is in a dynamic state where the rate of flow is changing. Some type of changing restriction downstream of the drop forming location is active.

In Fig. 3-1c the system is in a steady-state flow. The rate of flow is constant. Some type of restriction can be present and at least the 'background' resistance, resulting from the system tubing and parts itself is present.

Planning

The plan is to measure:

- The volumetric flow rate (mL/h)
- The volume transported (mL)

These two parameters combined with the external input about fluid type provide the information base for our regulating system.

3-2 Volumetric flow rate sensing

The drip chamber present in every IV administration set is typically used for degassing and flow measurement. In the most basic way, flow measurement is performed by the caregiver. He or she counts drops passing by in the chamber during a certain amount of time. The amount of drops, gives an indication of the flow rate.

This drop counting flow measurement transforms measurement of flow into counting of defined drops (drip chambers are manufactured in such a way that 1 ml equals 20 (macro drip) or 60 (micro drop) drops). The estimated volumetric flow thus depends on the accuracy of the drop volume and the duration of the observation. The requirements of ISO8536 [6] for the drop forming orifice define an accuracy with a margin of 10% drop volume at constant temperature. Counting the drops gives however a good indication of the short term volumetric flow rate.

In the literature study [11] multiple ways of flow rate measurement principles (some based on drop detection) are discussed. Capacitive drop measurement is marked as the most efficient, robust and low priced way of detecting drops in a drip chamber. One downside is the inherent low accuracy caused by the drop volume variation. This is however less of a concern because with most IV fluids some short term (<1 min [12]) variation in flow rate is acceptable. This section describes the design and analysis of a capacitive drop detection sensor.

3-2-1 Working principle drop detecting capacitor

The general principle of capacitive drop detection is based on change of permittivity of the dielectric medium in between the plates of a parallel plate capacitor (Fig. 3-2).

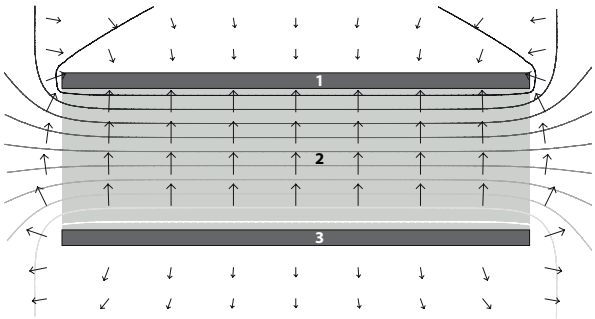

Figure 3-2: Cross section: Parallel plate capacitor electric field (arrows). Parts: 1,3 electrodes; 2 dielectric medium.

The capacitance of a parallel plate capacitor depends on the plates surface area '**A**', the relative permittivity '$\boldsymbol{\varepsilon_r}$' of the dielectric and the distance '**d**' between the two plates.

$$C = \frac{\varepsilon_r \varepsilon_0 A}{d} \tag{3-1}$$

where:

C = capacitance
ε_r = relative permittivity
ε_0 = vacuum permittivity
A = plate area
d = distance between plates

In the drop sensor design, this capacitor consists out of two curved plates (see Fig. 3-3) positioned on opposite sides of the drip chamber around the position of the drop forming orifice. The space in between the two plates forms the dielectric of the capacitor and consists of the wall of the drip chamber and air. Drop formation finds place in this space (Fig. 3-3b). At 20 °C the relative permittivity of water[1] is roughly 80 times that of air. As a result the permittivity of the dielectric between the two plates is increased during the growth of the drop. This change of permittivity results in an increase of the capacitance of the capacitor. Finally the aim is to measure this change of capacitance, as a measure for the drop growth.

Presumed optimal Signal to Noise Ratio (SNR) of the sensor is reached when the volume of the growing drop has the largest impact on the total dielectric volume of the capacitor. This can be accomplished by the correct dimensioning and placement of the two plates.

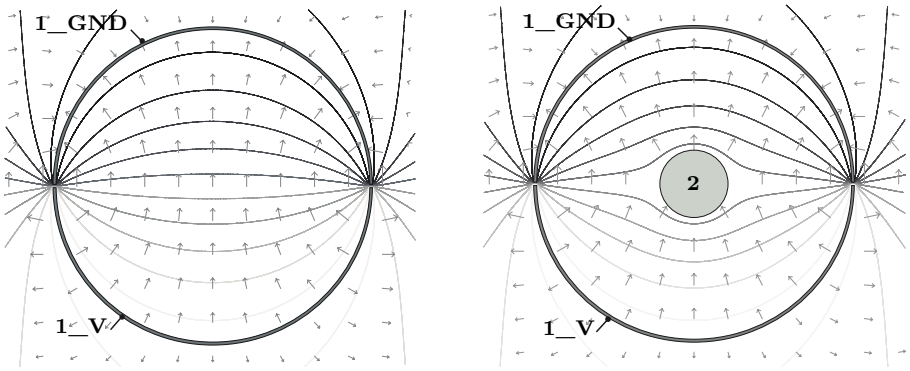

(a) Without drop **(b)** With drop

Figure 3-3: 2D FEM analysis of electrical field between two curved separated plates with applied potential. Numbered parts: **1.** Capacitor plate **2.** Drop

3-2-2 Implementation of sensor in the system

The two plates of the capacitor are attached to the outside of the drip chamber. The radius of the circle formed by the two plates is defined by the outer radius of the drip chamber. The variable dimension is the 'height' (direction perpendicular to plane viewed in Fig. 3-3) of the plates. A 3D view of the capacitor plates applied to the drip chamber is shown in Fig. 3-4, indicated is the variable height (**h**).

[1] Water can be used in experimental stage because IV fluids generally consists out of at least 90% water.

To be able to measure the change in capacitance, a capacitance to digital (C2D) converter is required. As mentioned, the **change** of capacitance is a relevant parameter for the detection of drops. The absolute value is of less interest. The C2D integrated in the NXP NHS3153 Integrated Circuit (IC) is used as converter. The measurement offset of the C2D in the chip is configurable from 0.1 pF to 4 pF in steps of 100 fF, the dynamic range can be set to 400 fF, 800 fF or 1 pF. This measurement range complies with the expected capacitance of 0 pF to 1 pF [13].

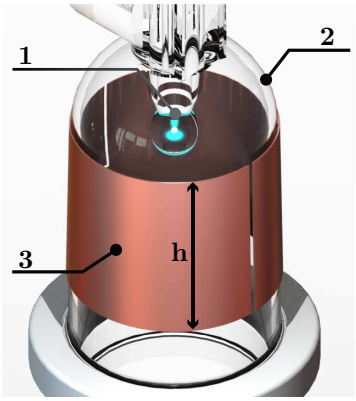

Figure 3-4: Rendering of capacitor plates applied to wall of drip chamber. Numbered parts: 1. drop forming orifice, 2. shell of drop chamber, 3. capacitor plate.

3-2-3 Measurement

A general test of the capacitor is performed by connecting the capacitor to the NHS3153 IC with separated wires of 10 cm. The drip chamber is set to slow dripping and the measurement is done at 14 Hz. The result of the raw capacitance measurement versus time is shown in Fig. 3-5. In the graph, the growth of two drops can be seen. The sudden change (the gray marked zones: 1) shows the detachment and fall of the drop. Zone 2 indicates the drop growth. At the points marked with **A**, the drop has reached its maximum size, and **B** marks the first measurement point after the fall.

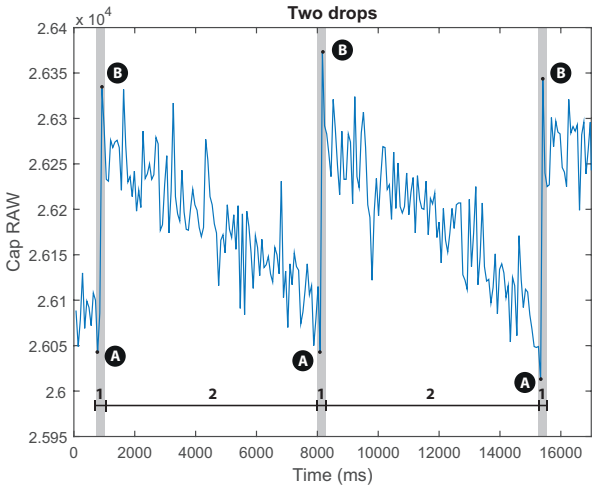

Figure 3-5: Two drops, dripping measurement

Remarkably, during drop growth there is a capacitance decrease. This is opposite of what was expected from equation 3-1. A theory for the explanation of this behaviour is discussed in 3-2-4.

Varying capacitor size (h)

To optimize the capacitors plate dimensions, multiple measurements with changing plate heights (h) are performed (Fig. 3-6). The upper part of the plates is positioned flush with the outlet of the drop forming orifice. The best performance were expected with a plate size that just encapsulates the region of drop growth.

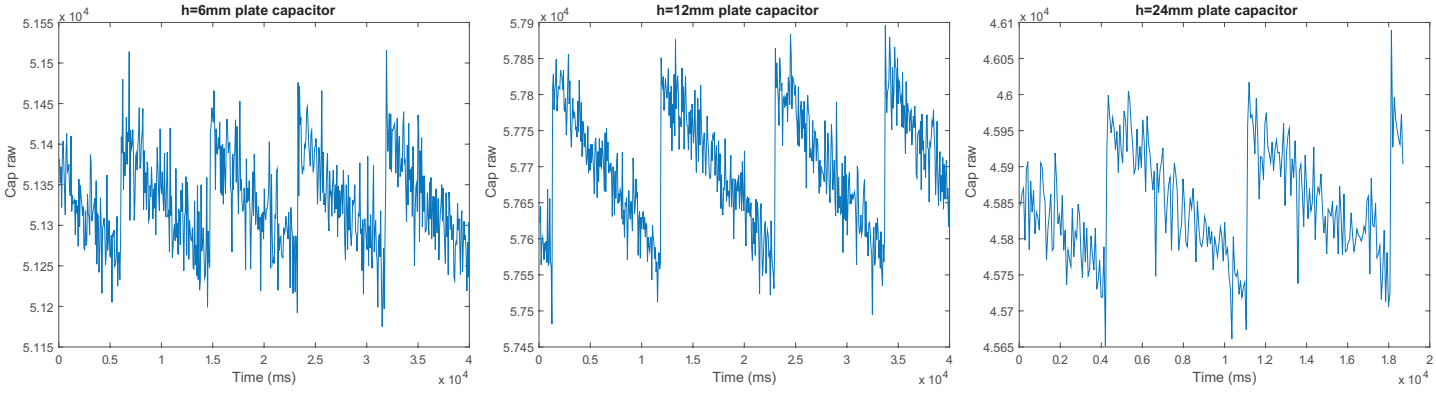

(a) Small capacitor plates **(b)** Medium capacitor plates **(c)** Big capacitor plates

Figure 3-6: Drop capacitance measurement with varying capacitor dimensions.

In Fig. 3-6 the measurement results are shown of the three experiments. The drip rate differs between the three experiments, resulting in a variance of the amount of measurements per drop. Although it should be possible to do a complete signal analysis and optimize the dimensioning, already sufficient information is available by first sight analysis:

1. Peak to peak raw values range from 300-350 (with 6mm cap on the low side)
2. Noise level of 6mm and 24mm capacitors is high compared to that of the 12mm capacitor

The first indicates that capacitance change is not affected by the size of the capacitor plates, as long as the full drop is completely encapsulated. The second that the SNR level is affected by capacitor size and has an optimum somewhere between 6mm and 24mm. The upcoming measurements are therefore carried out with the 12mm capacitor plates.

3-2-4 Error factors

It was expected that the drop growth, resulting in an increased replacement of air by water as dielectric, would increase the capacitance of the capacitor. The experiment however shows the opposite: during growth of the drop a reduction of capacitance is observed. To track down the origin of this unexpected measurement some differences between theory and the actual experiment were identified:

- Tap water is used during the measurement instead of pure water
- The measurement is done with a fast changing electric field
- The capacitor is not a parallel plate capacitor
- The drop is still connected during growth

It was initially unclear which differences were influencing the measurement. Multiple theories were proposed and tested to identify the root cause.

Theory 1: Influence of changing electric field & conductivity of tap water

The used C2D converter is based on a third-order differential delta-sigma convertor. Inherent on the working principle of this converter is the fast charge - discharging of the external (measured) capacitor. This excitation is done at a frequency of 1 MHz. The theory is that this excitation results in an interfacial polarization of the drop (Fig. 3-7a). This polarization combined with the conducting properties of tap water then forms a series capacitor. In this model, the drop acts as a conductor with a resistance. Parallel to this series capacitor stands a capacitor resulting from the plate to plate area around the drop (Fig. 3-7b).

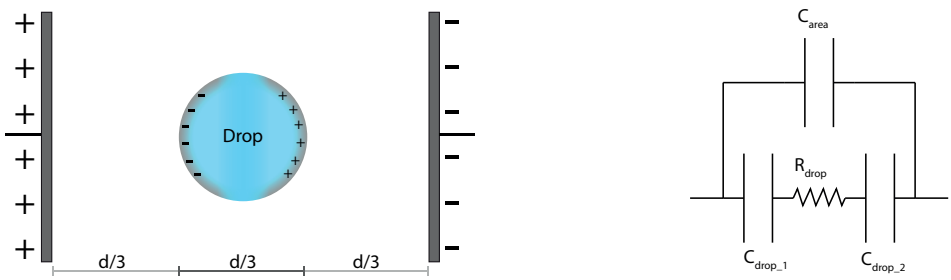

(a) drop model **(b)** equivalent model

Figure 3-7: Drop (dielectric) interfacial polarisation model

Considering for simplicity the situation where the distance between edges is $\frac{d}{3}$ as marked in Fig. 3-7a. The resulting capacitance is considered to be:

$$C_t = C_0 - \beta A + \frac{\alpha A}{2} \tag{3-2}$$

where:

C_t = resulting capacitance
C_0 = capacitance from area around the drop
A = plate area
α = in between drop and plate capacitance part
β = drop effect

In this theory the β effect has to outperform the α effect to decrease the resulting capacitance that is measured.

Testing the theory: If the conductivity of tap water is influencing the capacitance then testing with purified water would show the expected growth of capacitance. Therefore a measurement was performed with purified water[2]. The measurement was done by:

1. filling the reservoir with purified water
2. configure the roller clamp so dripping speed is $^1/_2$ Hz
3. measuring change in capacitance

Result & analysis: The measurement showed no clear capacitance change in either positive of negative direction. It seemed as if the drops had no influence on capacitance at all. To be sure that the setup was still functioning, the liquid was replaced by tap water while dripping. This made the reduction of capacitance to return. Either *alpha* and *beta* were perfectly equalizing each other, or some other factor was influencing the measurement. The expected increase of capacitance was still not measured.

Theory 2: Separating the drop from the reservoir

The model that was used for prediction the behaviour of the system presents the drop as an (2D) distinct entity. It is however still connected to the drop forming orifice and part of the liquid substance of the reservoir. The theory is that some electric charge flows away from the drop to the reservoir by ion flow, and that the change in capacitance is influenced by the fact that the drop is still 'connected' to the reservoir.

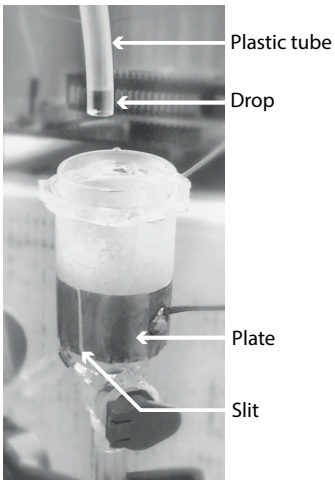

Figure 3-8: Test setup showing small tube filled with water and placeholder of drop chamber.

Testing the theory: To test the theory, a free floating drop between the plates would be ideal. As this is complicated to realize, a small plastic tube partly filled with water (tap and purified) is used (Fig. 3-8). The tube is used to be able to freely move the 'drop' of water.

The experiment is done three times: with purified water, with tap water and finally without water. Each time the process is:

1. suction of some liquid into the tube end
2. manoeuvre of tube end into the region between the plates
3. moving the tube in and out of the region
4. removal of tube

The test without water is done to check the capacitance change resulting from the tube material alone.

Result & analysis: While moving the drop in and out of the capacitor, a change in capacitance is measured (Fig. 3-9). The capacitance increases when the drop is moved into the capacitor region. This change is seen with purified and with tap water. The amplitude difference between purified water and tap water might be due to material properties but could as well be a result of a change of volume of the drop inside the tube. A slight increase of capacitance was seen during the measurement with the empty tube. This increase was roughly $^1/_5$ of the capacitance change of the measurement where a drop was present inside the tube.

This experiment clearly shows that the change in capacitance is different depending on whether the drop is still part of the liquid entity of the reservoir, or if it is separated. A theory how the reservoir has an influence on the capacitance change is discussed in the next paragraph.

[2] the possible contaminant levels of the used purified water were unknown

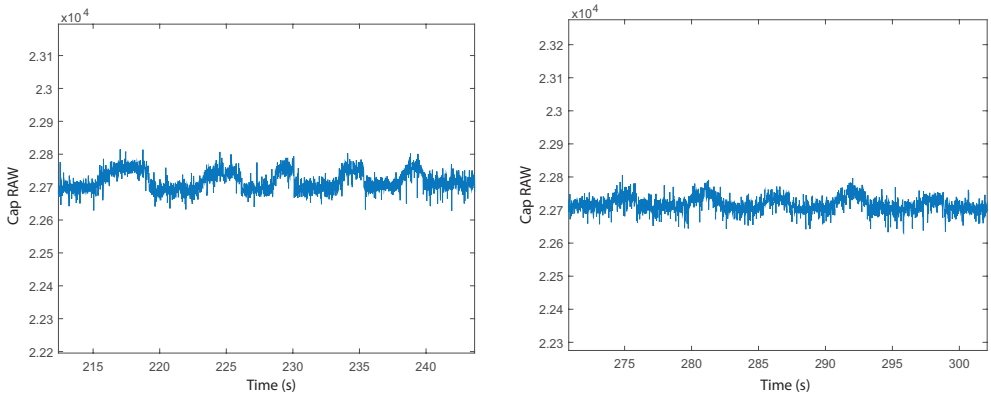

(a) purified water drop **(b)** tap water drop

Figure 3-9: Graphs of capacitance measurement while moving tube with drop in and out of region between capacitor plates.

Theory 3: Influence of reservoir "parasitic" capacitance

A third possible factor is an influence of the reservoir itself. A new theoretical equivalent circuit is drawn, shown in Fig. 3-10. In this circuit, the two capacitors ($C_{drop_{1,2}}$) formed by the drop are still present. A new capacitance in the circuit is C_{res}. This capacitor consists out of the liquid in the reservoir as one "plate" and another plate, formed by the surroundings to ground. R_{fluid} indicates the resistance of the water/IV fluid.

The theory is that during drop growth effectively C_{res} increases. This capacitance seems similar to a parasitic capacitance but has an different effect on the measurement: as C_{res} increases the charge buildup on $C_{drop_{1,2}}$ decreases. With a high enough value of C_{res} the C2D will effectively only measure C_{area}. This capacitance is small compared to the capacitance of the capacitor before the drop has entered the region between the two plates. The effect of the drop is equivalent to an area that is "taken away" from the capacitor without creating a charge difference at its edge.

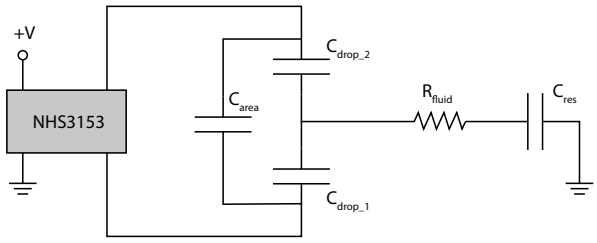

Figure 3-10: Circuit model of "parasitic capacitance ground drop" leaking principle.

Testing the theory: The theory is tested by building a circuit out of discrete components mimicking the expected equivalent circuit of Fig. 3-10. This circuit (Fig. 3-11) is used to experiment with different capacitance values of C_m. Two 2,2pF capacitors are used to

imitate the capacitance of the drop alone. Another capacitor (C_{int}) indicates the capacitance resulting from internal capacitance in the IC and the Printed circuit board (PCB).

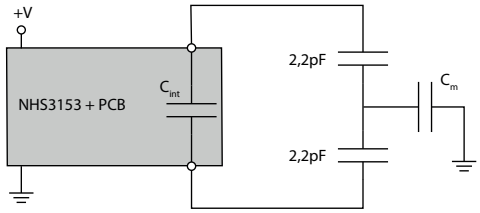

Figure 3-11: Circuit of experiment to test theory 3. C_m is varied.

The experiment is done multiple times, each time changing capacitor C_m with a capacitor of 0; 1,8; 4,7; 10; 15; 47; 150; 220; 330 pF. To measure C_{int} a measurement of capacitance is performed with nothing connected to the PCB pins. After this experiment the two series 2,2pF capacitors are soldered in place. At the centre, between the two capacitors, different C_m capacitors are soldered. The other terminal of the capacitor is soldered to the ground connection of the IC. Connections are kept at minimum length to minimize any parasitic capacitance.

Result & analysis: First a measurement of capacitance without anything connected to the PCB was performed, measured capacitance was 770fF. With the two 2,2pF capacitors connected, a capacitance of 1800fF (1100 + 770) was expected. The actual value that was measured was 1872fF. After these initial measurements, various C_m capacitors were soldered in place. The graph of C_m versus measured capacitance is shown in Fig. 3-12. A dashed (red) line at 770fF indicates C_{int}.

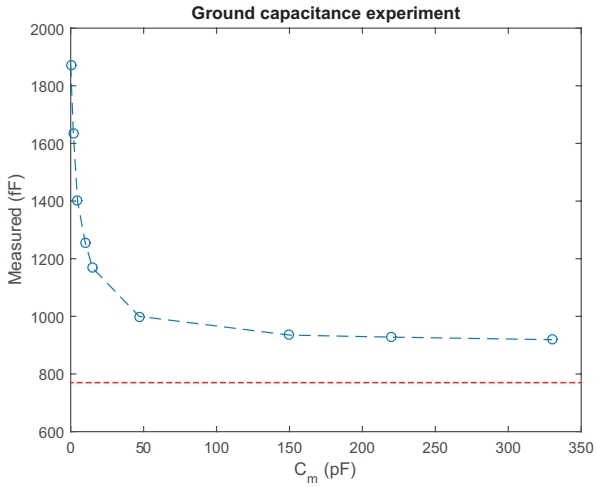

Figure 3-12: Graph of measured capacitance versus different values of C_m. Measurement points are indicated with circles. Dashed line indicates internal capacitance C_{int}.

The measurement clearly shows the reduction of measured capacitance when larger values of C_m are in place. Starting off with a large reduction in capacitance and stabilizing around 900fF. Expected was the "disappearance" of the two series capacitors. This is similar to the

effect that is measured, although a small offset of 200fF above 770fF can be seen. This offset is assumed to be the result of parasitic capacitance resulting from connections between the different applied capacitors.

Conclusion: The test circuit of theory 3 seems to mimic the behaviour of the actual drop sensor. The circuit shows that capacitance of the two assumed series capacitors 'resulting' from the drop, disappear when capacitor C_m is introduced. In theory 1 the use of purified water made the change of capacitance to disappear. This situation is not fully explained by the circuit of theory 3, but could be the result of C_m compensating for the two series capacitors ($C_{drop_{1,2}}$). The apparent influence of the ionic presence in the IV fluid and the connection of the forming drop with the IV fluid reservoir volume, might result in a complication of the detection of drops under various conditions (full/empty reservoir) and with various IV fluids.

3-3 Reservoir fluid level indication

Existing IV systems generally do not contain a system to measure the fluid level in the reservoir. They rely on measuring the amount of fluid that is transported and subtract that value from the initial volume of the reservoir. In the most basic way there is a measurement/check of the reservoir fluid level, namely an periodic check by the caregiver. Estimations of the fluid level are typically only used as an indication of the need for replacement of the reservoir. A direct[3] and regular measurement of the fluid level would however be a great indication for the supplied volume in the long term. Hereby the reservoir volume is converted from a necessary estimated parameter into an useful information containing parameter.

The literature research [11] provided two ways of directly measuring the amount of fluid present in the reservoir. One method is measuring the mass of the total system [14]. The other method uses Time-domain reflectometry (TDR) with two electrodes attached to the reservoir [15] [16] [17]. Both methods require intensive modification of the IV administration set. This section describes a sensor method that requires less modifications and can be integrated in a local regulating system attached to the drip chamber.

[3] with direct meaning directly related, independent of time

3-3-1 Working principle reservoir level sensor

Analysis of the administration set revealed that in the static no flow condition (see 3-1-1) the drip chamber is pressurized by the liquid present in the reservoir. The principle behind this raise of pressure is that at a certain depth in a fluid the pressure is:

$$P_{fluid} = \rho g h \tag{3-3}$$

where:

ρ = density of liquid
g = gravitational acceleration
h = fluid height above point

Translating this principle into the setup of the IV administration set (see Fig. 3-13): difference in pressure of the space inside the drip chamber and atmospheric pressure is related to the height of the water column (distance between point 1 and 2) above the drop forming orifice. Therefore measuring the pressure inside the drip chamber gives an indication of the fluid height in the reservoir above the outlet. Although fluid height is not volume, the parameter is still of interest: The actual shape of the reservoir determines the relation between volume and measured pressure/fluid height. The volume inside the reservoir is not necessarily linearly related to the pressure measured in the drip chamber. To be able to estimate the actual volume in the reservoir a certain "pressure profile" has to be made. This profile can then be adjusted with the two main boundary conditions of the system:

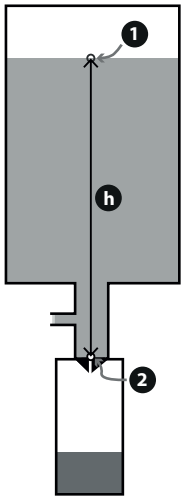

Figure 3-13: Water column height in reservoir indicated by 'h'.

- Initial liquid volume & measured pressure of reservoir at **start**
- Pressure inside the drip chamber at **end**

Both boundary conditions are known throughout the use of the system.

3-3-2 Implementation of sensor in system

The sensor should measure the pressure inside the drip chamber and transfer this pressure information to the NHS3153. Only the top $^2/_3$ of the drip chamber is filled with air. This is thus the preferred location for the sensor (schematically viewed in Fig. 3-14). It is possible to place the sensor either inside the drip chamber, or outside the chamber and connect it through the wall of the chamber. In case the sensor is placed inside

the chamber an absolute pressure sensor is required and if the sensor is placed outside of the chamber either a differential or absolute pressure sensor can be used.

As placement of the sensor inside the chamber is more complicated to realize, might bring contamination or sterility issues, and has no practical advantage, an externally connected sensor is implemented. This sensor is connected through the wall with the upper part of the drop chamber at the round edge above the outlet of the drop forming orifice (marked with nr. 2 in Fig. 3-4). This place is used because it reduces the probability of water getting into the tube connecting the sensor.

The expected pressure difference between a filled and empty reservoir of height 25 cm is:

$$\begin{aligned} \Delta P &= \rho g h \\ &= 1000 \cdot 9,81 \cdot 0,25 \\ &= 2452,5 Pa \end{aligned} \tag{3-4}$$

Measurements will be performed with the use of a NXP MPL3115A piezoresistive absolute pressure sensor [18]. This sensor is able to measure pressure in a range of 50 kPa to 110 kPa with a resolution of 1.5 Pa and a relative accuracy of 50 Pa. Translating this into properties of the IV administration set: it can measure the expected pressure difference between full and empty reservoir (103 778 Pa to 101 325 Pa) with steps of 0.1 mm and an accuracy of 5 mm. Communication with the sensor will be via I2C with the NHS3153, an example of the communication code is given in appendix C-1. The sensor is placed on a breakout PCB (shown in appendix B-1) to interface with the pins of the IC and connect essential external components.

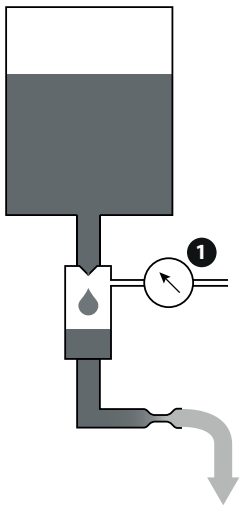

Figure 3-14: Schematic indication of pressure sensor location.

3-3-3 Measurement

The functional principle of measuring the fluid volume by pressure difference is tested by an experiment where the pressure was measured during emptying of an IV fluid bag with tap water, the test setup is shown in appendix B-2. The ideal experiment would be to:

1. completely fill the reservoir
2. drain reservoir by infinite small amount
3. wait till pressure stabilizes
4. measure the pressure
5. start again at 2

This is practically impossible as the reservoir is drained continuously. The pressure measured is thereby no longer only influenced by the water column in the reservoir. A pressure drop due to tubing resistance and the outflow will influence the measurement. Both are assumed to be constant offsets at the used low flow. The experiment is performed three times, results are shown in Fig. 3-15. During this experiment a differential pressure sensor was used (NXP MP3V5004GC6U [19]) attached with one port through the wall of the drip chamber.

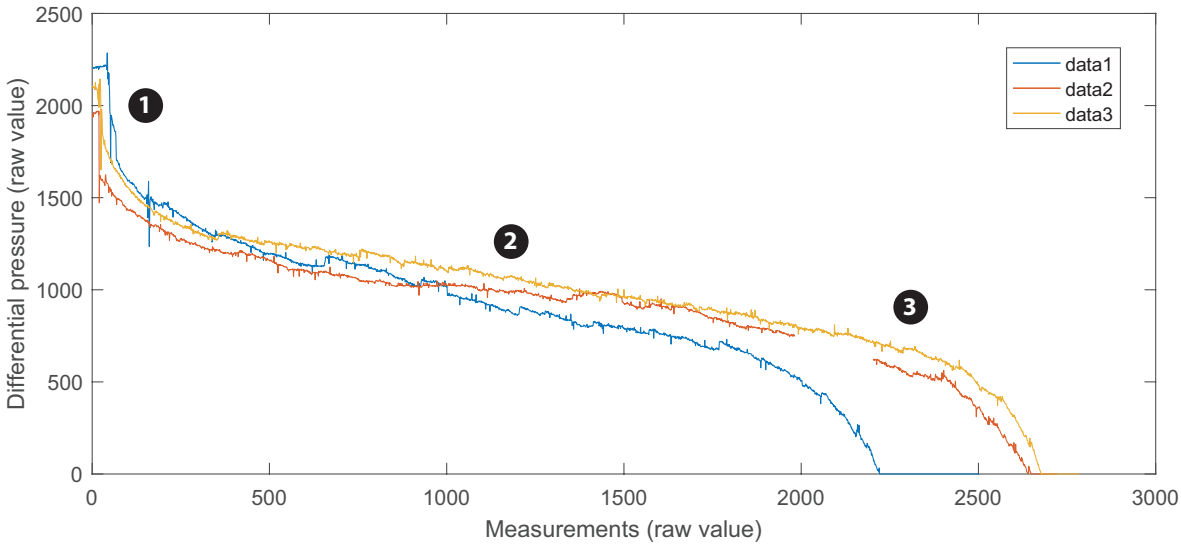

Figure 3-15: Three differential pressure measurements of emptying an IV bag reservoir from full. The gap in one of the measurements is the result of lag in data logging.

Different stages

The measurement shows that the pressure (difference) reduces during emptying. The profile can be split up into three stages (marked by 1,2,3):

1. nonlinear reducing decrease rate
2. stable linear decrease rate
3. nonlinear growing decrease rate

It is assumed that this profile is the result of the shape and material of the IV reservoir bag: During the first stage the bag is completely filled with liquid. The plastic material of the bag is stretched and pressures the liquid initially. As the bag is emptying it becomes relaxed, in the second stage the liquid flows out by atmospheric pressure and mass. During this stage the bag deforms easily and has minimal influence. In the third (last) stage, pressure reduces at an increasing rate. When the shape of the bag (Fig. 3-16 a) is analysed it can be seen that the width of the reservoir reduces in the bottom part. When outflow is kept constant, the water column height (and thus the measured pressure) in the centre will decrease at an increasing rate.

(a) IV bag (Baxter) **(b)** IV vented bottle (B. Braun)

Figure 3-16: Two types of IV reservoirs

Profile shape

The pressure profiles of the three experiments are each a bit different. Experiment data 1 (blue) starts with the highest pressure difference and ends the first. Data 3 (yellow) starts in between the two other experiments and takes the longest time to empty. Also the slope of the pressure measurement is different between the experiments. These differences are due to different start capacity[4] and drip rate settings. These profiles are remarkably similar to battery discharge profiles (Fig. 3-17). Estimations of battery capacity and discharge rate is thoroughly researched and multiple models are available. The input parameters in the IV reservoir situation are starting volume and empty reservoir pressure, both known. These, combined with later measurements, can be used to fit a curve to the measurements and predict flow rates on the long term.

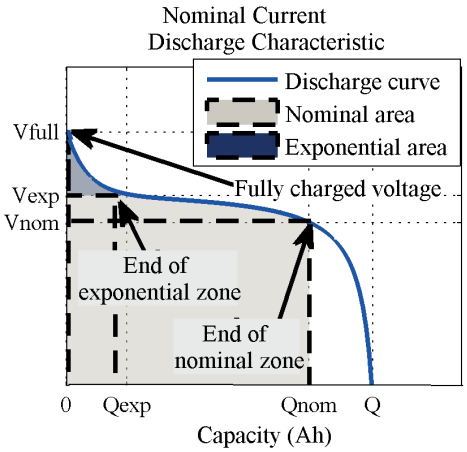

Figure 3-17: Typical battery discharge curve (from: O. Tremblay 2009 [20])

[4]the reservoirs were manually filled and some differences in total volume were present

3-3-4 Error factors

Reservoir type

Before the measurements shown in Fig. 3-15 that uses an IV bag as reservoir, a measurement was performed with an 500 mL B. Braun Ecoflac®. The Ecoflac/bottle requires the uses of a vented system because deformation of the bottle is limited. This system consist out of a small venting port present in the needle of the drip chamber. Inside this port is a one way valve created by a fine gauze. This gauze prevents water from leaking out, filters incoming air and makes outflow of water possible by replacing it with air. The resulting profile of this experiment is shown in Fig. 3-18.

Use of a vented system has a big influence on the pressure measured inside the drip chamber. During emptying the process can be split up in multiple stages (Fig. 3-19) being:

1. outflow of fluid is started
2. reservoir is deformed and under pressured
3. under pressure of reservoir breaches one way valve, air enters
4. reservoir empty but still deformed, air continuous to flow in
5. reservoir internal pressure equal to outside pressure

These stages deform the relation between pressure and fluid column inside the reservoir, making it impossible to use a pressure sensing method for prediction of reservoir fluid volume. This sensing method is therefore only applicable to administration sets that make use of non-vented IV bag reservoirs.

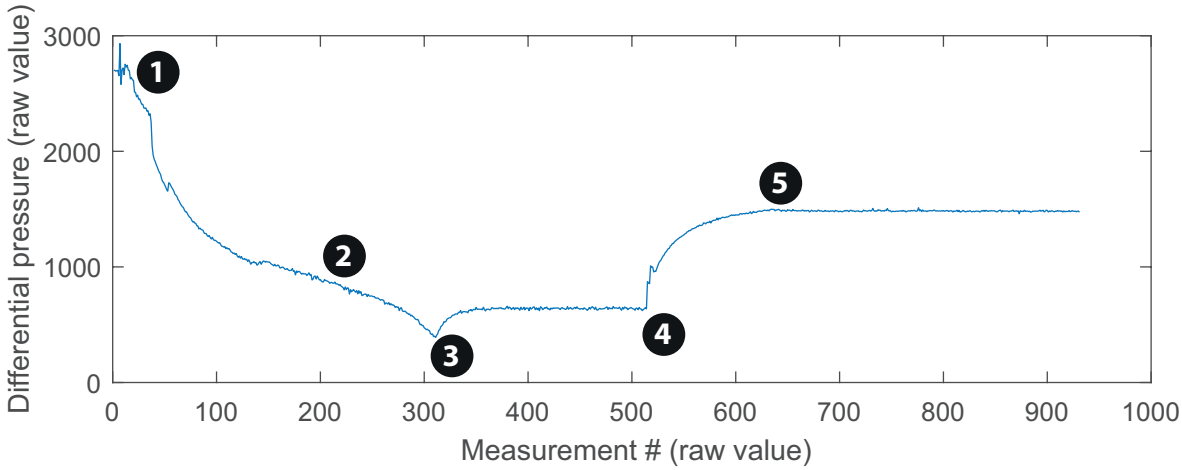

Figure 3-18: Differential pressure measurement of full to empty vented IV bottle.

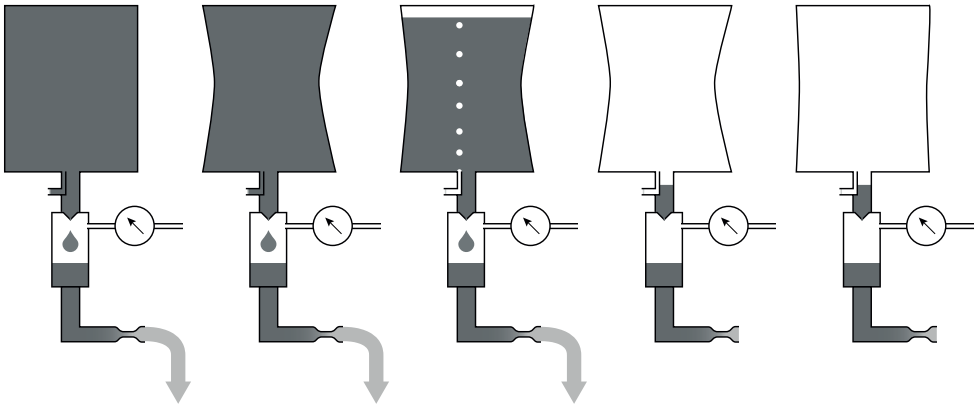

(a) 1 - outflow start

(b) 2 - under pressure reservoir

(c) 3 - breached vent

(d) 4 - under pressure empty reservoir

(e) 5 - stabilized empty reservoir

Figure 3-19: Schematic view of stages of bottle pressure measurement

Chapter 4

Actuator - Valve design

4-1 Introduction

Improving the regulation method for gravity based Intravenous (IV) starts by the indication of requirements and limitations of the existing system. The typical IV administration set uses a roller clamp for the regulation of flow (as discussed in section 2-3-1). The roller clamp is designed for manual operation and not for automated regulation. It alters the flow resistance of the tube by adjusting its inner diameter, this is accomplished by deformation of the tubing material (see section 2-3-1). This method of flow regulation leads to its two main disadvantages: inefficiency and slow response. The method is inefficient, because most energy required for flow regulation goes into deformation of the tubing material. The slow response is the result of indirect influence on flow resistance. When the roller is repositioned, the tubing material takes some time to settle in response to (restoring from) the deformation. This results in a time lag between positioning and effective flow adjustment.
Both of these disadvantages are not a limiting factor for manual control. The reason for the use of this clamp design is (besides low cost) the low risk of bio contamination: Flow can be regulated without creating a connection between inner and outside of the tubing system. The simple design, consisting out of two parts, facilitates sterilization. A technique for flow control that enables automated regulation, should combine this low bio contamination hazard with a faster controllable flow regulating mechanism. Summarizing the essential and more general requirements for the system:

- preservation of sterile environment in administration set, during regulation
- sterilisable valve mechanism
- flow rate regulation from 0 - 100%
- static holding position
- potentially powered from battery

- device cost in range of existing devices (2-15 dollar)
- minimal modification of existing administration set

The following sections describe a new method (patent pending by NXP) of flow regulation that complies with the summarized requirements. Separate sections describe the actuation mechanism and the valve mechanism. The valve mechanism embodies all parts that directly influence the flow rate. The actuation mechanism describes the actuator and the principle of actuation of the valve plunger. The chapter concludes with a description of the functioning of the designed mechanism, during tests.

4-2 Valve mechanism

Existing flow regulation devices regulate flow by either acting on, or between the tubing of the administration set. The devices that act on the tubing does not come in contact with the IV fluid. The presented valve mechanism is located inside the drip chamber and is thereby in direct contact with the IV fluid. The actuation of the valve (described in section 4-3) is however realized without the need for a connection through the hygienic protecting barrier created by the administration set.

The outlet of the drip chamber is made of non-flexible plastic that functions as a funnel for IV fluid. It also serves as a support fixture for the connection of the tubing to the drip chamber. The flow regulating valve is created by combining a (new introduced) conical shaped needle (Fig. 4-1) with the existing chamber outlet. This combination forms a needle valve type design (Fig. 4-2). The plunger assembly slides along the walls of the drip chamber, in and out of the outlet while it is supported by a perforated upper guiding ring. The valve is open when the needle is in the upper position and closed when the pin completely fills the outlet. The pressure drop resulting from the constricted space formed by the needle, varies depending the position of the needle. The pressure drop in open position is minimal as fluid is not obstructed by the needle and can easily flow through the holes in the perforated upper guiding ring. Different rates of flow can be realized by setting the pin at intermediate positions. A ring at the centre of the plunger assembly functions as end stop and plugs the outlet.

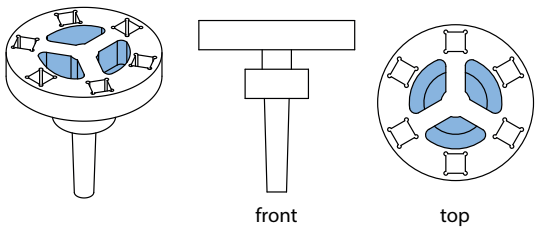

Figure 4-1: Valve needle assembly with gray/blue indicating the fluid passage holes in the upper supporting ring.

The valve design profits from the existing design of the drip chamber. Only minor modifications of the chamber are required to implement the valve. The gauze filter that is fixed to

the outlet of the drip chamber (see section 2-3-1) is however removed to make room for the needle and should be reintegrated at a different location in an actual device.

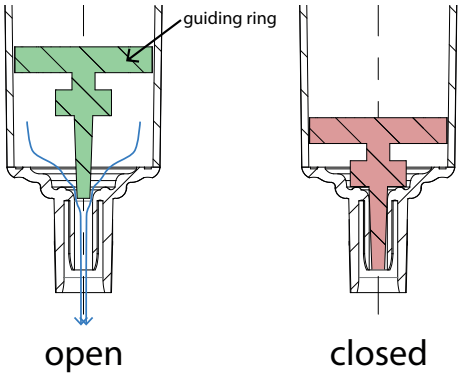

Figure 4-2: Cross-section of valve in open and closed position, arrows indicate fluid path.

4-3 Actuation

The actuation of a valve generally requires a mechanical coupling from the outside to the inside of the system. A conventional needle valve approach would therefore require a direct connection through the drip chamber wall to actuate the plunger of the valve. This is however a undesirable construction, as preservation of sterile inner system is one of the requirements of the valve design. To preserve the inner sterile system, actuation of the inner plunger is accomplished by making a magnetic link with the outside system. This coupling technique, for the actuation of material in an enclosed system, is also used in for example vacuum chambers and dishwasher pumps.

4-3-1 Magnetic linkage

The linkage system consist out of two rings: one ring is positioned inside the chamber, the other ring is positioned around the chamber. The inner ring is part of the plunger assembly and also guides the conical pin. Its diameter is smaller than the inner diameter of the chamber, in both closed and open positions (see Fig. 4-2). The outer ring can slide in vertical direction around the chamber and is positioned at the same height as the inner ring. Integrated in both rings are six cubic formed magnets (see Fig. 4-4 and appendix B-3). The poles of these magnets are placed side by side in an alternating configuration and opposing in inner and outer ring. This configuration magnetically couples the outer ring to the inner ring. Altering the position of the outer ring thereby results in a change of position of the inner ring and thus of the attached plunger.

The geometric configuration, strength and polarity of the magnets forming the link is chosen such that the link is stronger than the frictional force resulting from the plunger assembly sliding along the chamber wall and outlet. The used configuration of alternating magnets in the horizontal plane is however more suitable for transferring rotational forces. This setup is chosen for the ease of fabrication, a more optimal configuration for vertical movement is

shown in Fig. 4-3. This configuration can be combined with the existing horizontal alternating magnet setup to create a firm link in both (horizontal and vertical) directions.

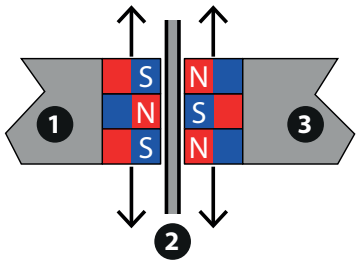

Figure 4-3: Vertical section view of optimal configuration for vertical movement of magnetic link. Indicated with N and S are the pole configurations of the magnets. Numbers: 1. inner ring, 2. chamber wall, 3. outer ring.

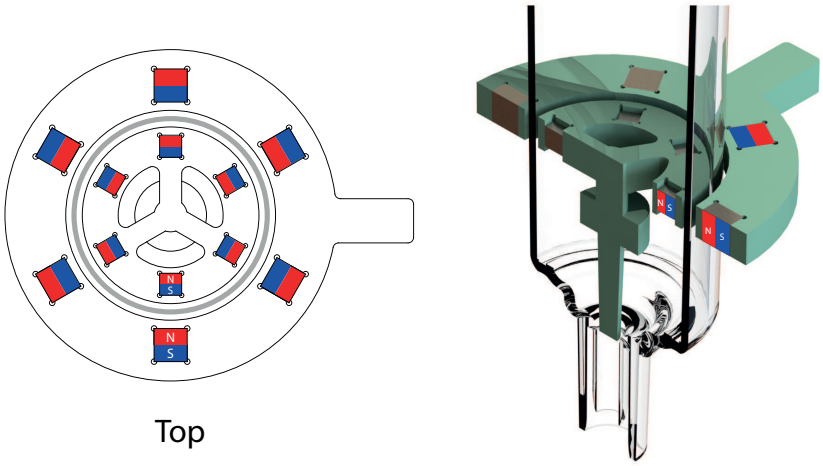

Figure 4-4: 3D section view of pin valve magnets and outside actuation ring. Marked with red and blue are the north and south poles of the magnet.

4-3-2 Actuator

One advantage of the valve mechanism is that the force required for actuation, consists (for the greater part) out of frictional force resulting from the plunger and the linkage mechanism. This force is relatively small compared to the force required for actuation of a clamping device. Controlling the valve is accomplished by vertically displacing the outer ring. The displacement is accomplished with use of a linear actuator. The described construction and material used for the actuation of the valve are optimized for the materials and construction techniques that were available. The described actuator mechanism is one out of many possible options for actuation of the outer ring.

The linear motor used for actuation of the mechanism is a commercial available servo motor with linear gearbox [21]. The motor and gearbox are fixed together on a Printed circuit board (PCB), forming a compact assembly. The servo assembly is attached to the outlet of

the drip chamber by a plastic socket which aligns the output pin of the gearbox with the protruding part of the outer valve ring (see Fig. 4-6). The outer ring is connected to the output pin by a vertical bar.

The position of the servo is controlled by a pulse width modulated (PWM) signal with 50Hz cycle time (see Fig. 4-5). The duty cycle of the PWM signal controls the position of the output pin. The plunger (that is linked to the output pin) can thereby be set in open/closed position or anything in between. The generation of the signal is accomplished by activating a 50Hz timer of the NHS3153 (example code in appendix C-3). The period of the timer is 20ms, during which it counts from 0 to 9999. The position of the servo is set by switching the output pin from low to high during the end part of the period (the switching moment is indicated by a number in the code between 0 - 9999). The signal is reset to low at the start of a new period. The duration of the 'on time' (duty cycle), signals the servo to regulate to a specific position.

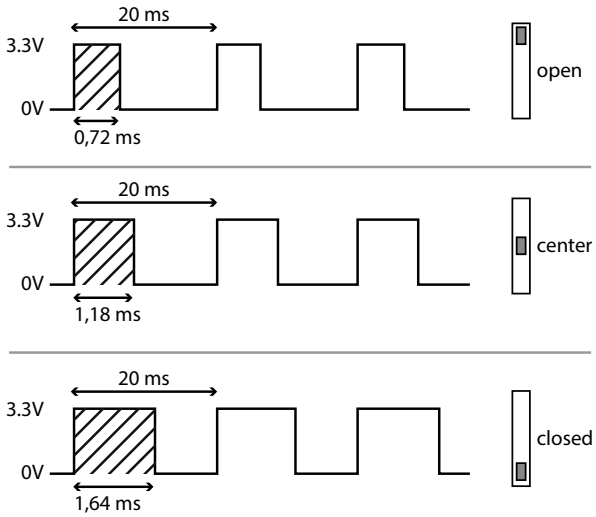

Figure 4-5: PWM duty cycle and corresponding actuator position (pulse is not to scale).

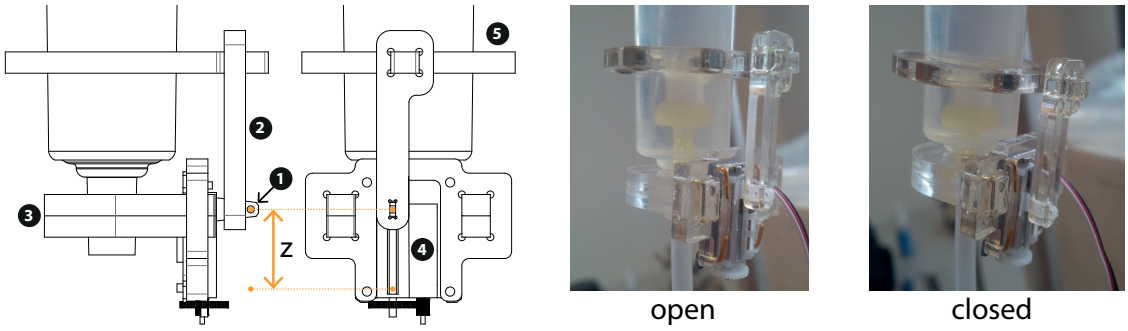

Figure 4-6: Open and closed position of valve with indicated the corresponding servo position (z), numbered: 1. servo output pin, 2. linking bar, 3. servo socket, 4. servo + gearbox, 5. outer ring.

4-3-3 Test and conclusion

Both the valve mechanism and method of actuation principle are, according to visual inspection during tests, able to perform their appropriate tasks. The magnetic link was able to keep the inner ring in position with the outer ring and different servo positions resulted in a change of flow. The system was also able to keep a static holding position when it was not actuated, a result of friction in the drivetrain of the linear servo assembly. Multiple deficiencies were however also noted:

1. Flow of liquid was still present when the valve was in closed position.
2. The plunger moved in a slip-stick motion during actuation
3. The link between the servo and outer ring was not rigid

The described deficiencies are expected to be the result of the rough manufacturing techniques used for fabrication of the parts. The performed test functioned as a proof of principle of the valve and linkage mechanism. A test of the performance of the system has been carried out by combining the regulator with the sensors described in chapter 3. The results of this test are discussed in chapter 5. The separation of the valve mechanism into an internal and external part, makes the system to comply with three critical requirements. First: The entire flow system, from reservoir to patient, can be kept enclosed during regulation, preserving the sterile IV flow. Second: The plunger part is sterilisable and can be sterilized together with the administration set. Third: The modification of the administration is kept minimal by the addition of a plunger and externally attached actuator. The material cost of the described system are approximately 7 dollar (servo $4,5 + magnets $1,5 + various plastic parts $1,-). These costs do not include the various other system parts (sensors, logic and housing), but are expected to reduce by mass production.

Chapter 5

Integration

5-1 Introduction

The preceding chapters described the different parts that could improve the control of a gravity based Intravenous (IV) system. The power of a regulated system lies in the way the information and method for actuation, presented by these parts, is combined. This chapter starts with the results of tests performed with the combined parts and concludes with a possible way for the implementation of a regulated system.

5-2 System tests

The aim of the two sensors is delivering information about the short and long term flow rate (see section 2-1). The following two sections describe a test of the functioning of these sensors when combined with the developed actuator. All tests are executed with a test configuration shown in Fig. 5-1 (in appendix B-3 the sensor/actuator assembly is shown). The LPC Link2 is used for debugging of the NHS3153. The MPL3115A2 communicates with the NHS3153 via I2C, processed information is split up and sent from the NHS3153 to the Arduino. The Arduino recombines the received information (see appendix D) and serves as a I2C to serial port for the PC. The PC receives the information of the serial port, from which further logging and processing is possible. The setup with the Arduino is used because of the absence of an easy debug out option in the NHS3135 SDK.

5-2-1 Long term flow test

The rate of the long term flow is to be deduced from the change in pressure resulting from the fluid head of the reservoir. In section 3-3-3 a measurement of the pressure change in the drip chamber during continuous emptying of the reservoir is described. A system in actual use has

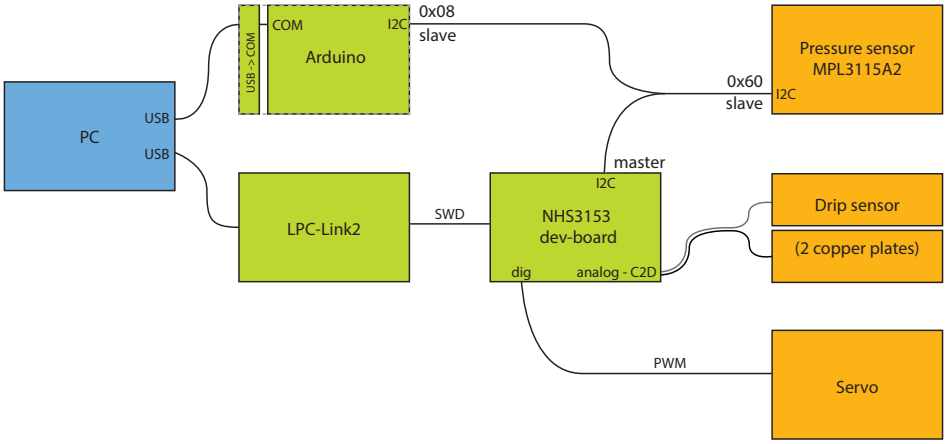

Figure 5-1: Test configuration for sensor actuator system. The lines show the links between the different components and the used communication protocols.

to measure the pressure with a closed valve to rule out any influence of 'lower'[1] components. Therefore a test is performed that has a continuous routine with the following steps:

1. close the valve
2. stabilize the system for a couple of seconds
3. repetitively measure the pressure
4. open the valve for a certain period of time

- repeat at 1

The test starts with a 1L tap water filled reservoir and ends when the reservoir is empty. The results of this test (see Fig. 5-2 shows a pressure changing profile, similar to the result in section 3-3-3. The measured 'noise', is the result of a stabilization period that is too short: pressure in the drip chamber was still rising when repetitive measurements were performed. The test shows that the measurement of pressure inside the drip chamber gives valuable long term information about the volume present in the IV reservoir.

5-2-2 Short term flow test

The information for short term regulation is deduced from the dripping rate. The test makes use of both the long term and short term flow rate sensors combined with the actuator. The flow of the test program is shown in Fig. 5-3 and the corresponding firmware code for the NHS3153 is shown in appendix C-4. The program opens and closes the valve in small steps during which constantly the capacitance of the drip sensor is measured (C2D routine). The C2D converter of the NHS3153 is able convert at a rate of approximately 62Hz at 15bit resolution. This property is used in the routine by the implementation of a 1 second delay

[1] lower from reservoir to body, following the IV fluid through the system

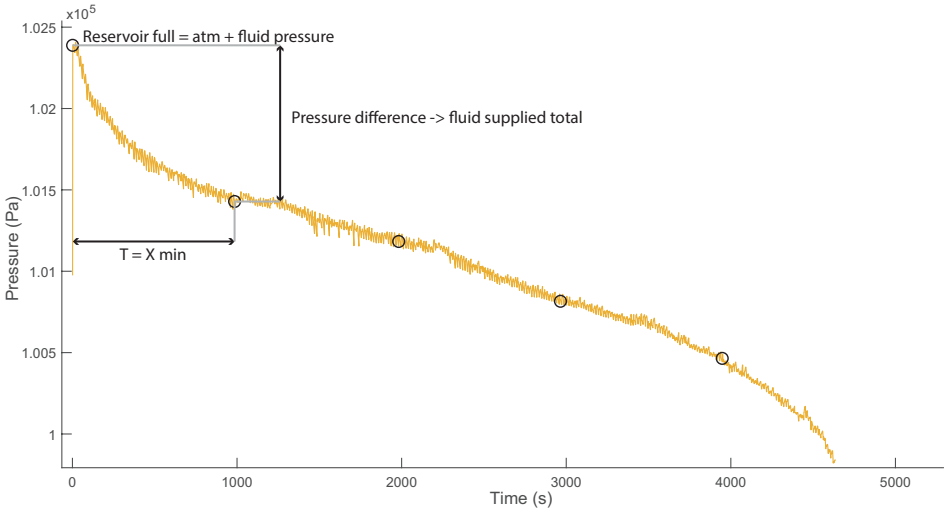

Figure 5-2: Pressure log of experiment with periodic valve opening.

consisting out of 62xC2D conversions. A pressure measurement is conducted when the valve is closed. During the full length of the test a roller clamp is applied to the IV tubing, that increases the flow resistance.

The logged data of three times closing and opening of the valve (resp. 0-100% PWM) is shown in Fig. 5-4. The plotted capacitive measurement data, is smoothed with a Savitzky-Golay filter in Matlab to facilitate peak detection (see appendix E)

Peak detection is conducted on the negative peaks as the abrupt drip of a drop, results in a isolated peak. The peak detection is performed by configuring the minimum distance from peak to peak and the minimal change in value in the region around a peak into the peak detection function of Matlab.

The distance from peak to peak ('diff(locs)') is used for the calculation of the drip rate. The dripping rate is shown in the third plot. A readout shows a maximum dripping rate of approximately 2Hz. During opening of the valve multiple abrupt changes in dripping rate are measured. This corresponds to the noticed slip-stick effect of the valve in earlier experiments. Closing of the valve results in a more gradually decreasing dripping rate. Some delay is shown between the actuation of the servo and flow rate change. This is observed to be partly caused by the lack of rigidity of the link between the servo and the outer ring, and partly by slack present within the magnetic link.

At four instances during the 17,5 minutes of the test, the pressure inside the drip chamber is measured. These are the moments that the valve mechanism is in the closed state and the change of pressure is solely originating from the changing fluid head in the reservoir. The readouts are plotted in the bottom graph and show a gradually reducing pressure, matching with a reduction of the fluid volume inside the reservoir. A more qualitative analysis of the pressure difference could be made, if the amount of fluid administered by the system is simultaneously measured by a reference system.

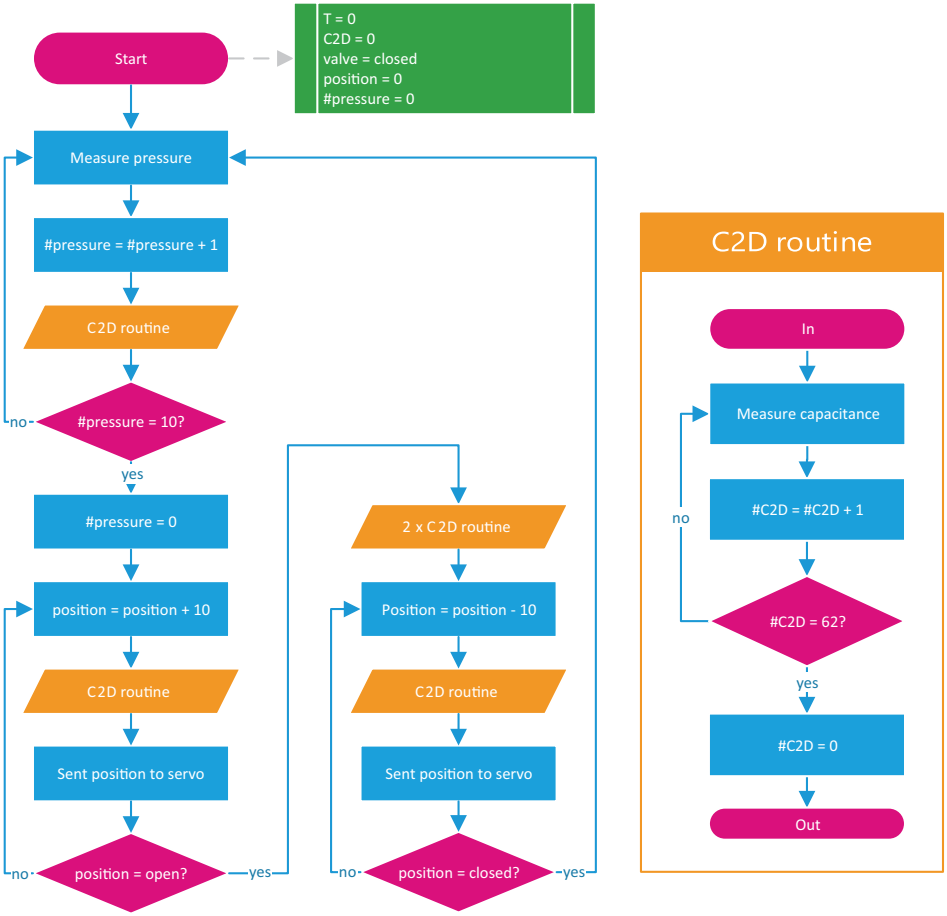

Figure 5-3: Program routine for testing the short term flow measurement and control

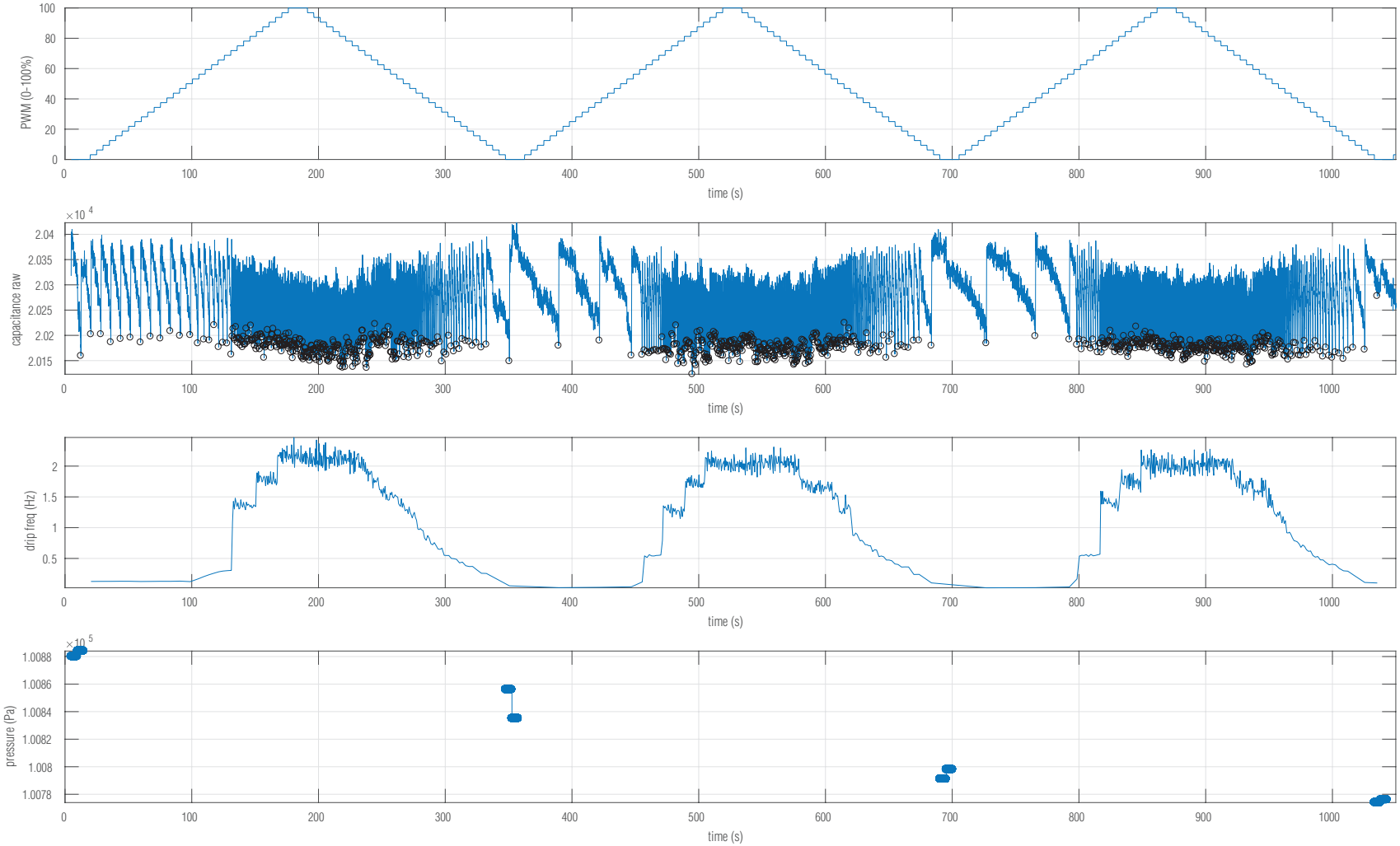

Figure 5-4: Short term flow sensor and actuator test. The first graph shows the PWM position information sent to the servo. The second graph shows the raw capacitive value with peak detection (circles). The third graph shows dripping frequency (1/peak to peak distance). The bottom graph shows pressure measurement with the valve closed.

5-3 Routine for a regulated system

A possible way for the regulation of the IV system is presented by the state diagram shown in Fig. 5-5. This system uses the best known initial parameters to start regulating, after which it tries to optimize these initial parameters by newly measured information.

5-3-1 Initial regulation

The system starts by measuring the initial pressure. This defines the starting point of the pressure profile that can be used for the prediction of the reservoir fluid level. The second step is setting the valve to a position that is assumed to result in a flow of the desired rate. The opening of the valve initiates a flow of fluid through the drip chamber. The dripping drops, with an assumed volume of $^1/_{20}$ or $^1/_{60}$ mL, are counted during a specific time frame. The position of the valve is adjusted if the measured flow[2] does not correspond to the configured rate.

5-3-2 Continued regulation

After a certain amount of time 'T', a pressure measurement is conducted (with closed valve). The measured pressure combined with the initial and other pressure measurements, gives an insight into the rate of volume change in the IV reservoir. An example of these measurement moments is indicated by the circles in Fig. 5-2 on page 41. The volume change during the time window 'T', is subsequently used to recalculate the actual volume of the drops counted. A new drop volume is thereafter set for further regulation in the next time window. A possible measured deviation of the flow rate on the long term can be compensated by adjusting the valve's position during the new time window.

The pressure measurement is used by this system as a periodic correcting factor for flow delivery that is controlled by drop counting.

[2] equation: $\frac{drops \cdot dropvolume}{time}$

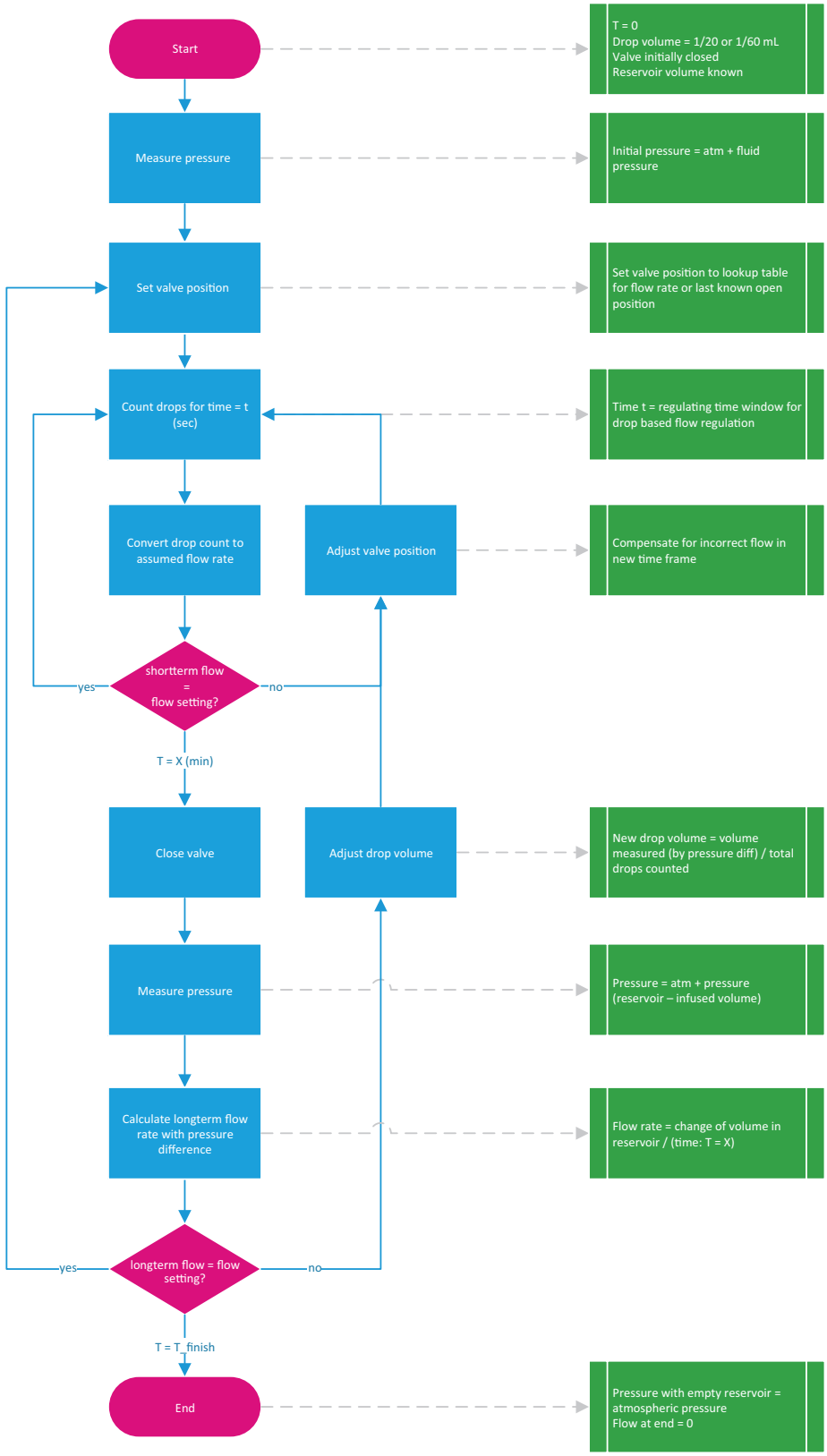

Figure 5-5: Flow chart for system regulation with the use of long and short term flow sensors.

Chapter 6

Conclusions and Discussion

This chapter presents the conclusions of this research study and provides recommendations for further research into the regulation of gravity based Intravenous (IV) therapy. Furthermore, in section 6-2 are some points of attention for the presented information.

6-1 Conclusions

The existing IV administration techniques cover the brought range of use for IV therapy. However, a gap does exist when performance and cost of the different techniques is laid out. This gap is located between, on the one hand the passive techniques that are low priced and low performing, and on the other hand the active devices that are expensive and have a high performance. The focus of this thesis is the research into a new IV administration technique that fits in 'the gap'. The main research question is formulated as:

> What kind of sensing and regulating method can be used to improve the control of gravity based Intravenous (IV) therapy?

In this study a sensing and regulation method is developed by dividing the method into three main parts, namely a:

1. sensor method
2. actuation method
3. regulation method

The following paragraphs present the conclusion following from the development of these three methods.

Sensor method The existing methods for flow rate sensing are analysed in chapter 2. They are based on the counting of defined drops by the caregiver. Drop counting gives a great indication of the rate of flow on the short term. Therefore a sensor is fabricated, as discussed in section 3-2, that is able to detect the drops, dripping inside the drip chamber. This sensor consists out of two curved copper plates. A capacitance to digital (C2D) converter is used to measure the change of capacitance resulting from the drops, dripping between the plates. A distinct sawtooth signal, corresponding with the dripping drops, is measured by the sensor.

As the volume of the drop is subject to variation, drop counting alone is not an accurate method of flow rate sensing on the long term. To be able to measure the flow rate on the long term, a new measurement method is presented in section 3-3. This sensor gives an indication of the volume inside the IV reservoir by measuring the pressure inside the drip chamber, resulting from the fluid level head of the reservoir. Only flexible reservoirs can be used with this sensor as vented administration sets unpredictably affect the pressure. Performed measurements show that the pressure inside the chamber changes according to a distinct recurring three stage profile.

Actuation method A new valve design for the regulation of IV flow is developed in chapter 4. The existing flow regulators in use for gravity based IV function by a clamping technique. This technique is not optimal for automated regulation. The presented valve regulates the flow by constricting the size of the output port of the drip chamber with a needle shaped plunger. A mechanical coupling is created to manipulate the position of the plunger inside the drip chamber without breaching the sterile environment of the inner fluid system. Tests show the functioning of the valve design: flow rate is adjusted by changing the position of the plunger and the plunger follows the poscition of the outer ring due to the magnetic link.

Regulation method A method for the regulation of an IV regulator that makes use of the developed sensors and actuator is presented in chapter 5. By detection of peaks in the sensor data of the drop sensor, the drip rate can be calculated. The volume of the drop, used for direct flow regulation, is adjusted by periodically measuring the total volume infused by the system. Further research is required to test the performance of this model.

Recommendations

The definition of a specific flow rate and accuracy for an IV therapy, aim at accomplishing a certain clinical outcome. Better definition of the clinical relevance of the accuracy of flow, required for multiple types of IV would increase ability to design and optimize a regulating device for more specific needs of certain therapies. The link between clinical outcome and technical requirements should therefore be better defined.

The information of the pressure sensor is only used for the sensing of fluid level in the reservoir. Continuous measurement of the pressure during flow of the IV fluid could contain more information about the condition of the patient. The opening of the valve creates a direct connection between the circulatory system of the patient and the IV administration system. Back pressure of the vein can potentially be sensed in the drip chamber and contain information about, for example the heart rate.

The designed valve mechanism uses an up and down sliding movement of the plunger to adjust the rate of flow. A redesign of the plunger could facilitate a construction in which the plunger rotates. This would potentially solve the slip-stick behaviour of the valve and reduce the valve assembly size.

The used drip peak detection method could be optimized by implementing a system that calculates the average of the signal (within a time window) and detects crossing of this average (with a minimal neighbouring distance). Such an algorithm can be integrated in the controlling Integrated Circuit (IC).

6-2 Discussion

The described reservoir fluid sensor, measures the pressure resulting from the fluid head in the reservoir. With this setup, any deformation of the reservoir potentially results in a change of the fluid head and thus of the measured pressure. The effect of deformation and type of reservoir bag, should be tested to gain insight into the accuracy of the sensing method that uses pressure for the estimation of reservoir fluid volume. Another point of remark is the lower then atmospheric pressure measured during tests. This is unexpected behaviour as it was expected that the system at rest would stabilize around atmospheric pressure. A possible, not verified, reason for this is that the fluid in the IV tubing underneath the drip chamber reduces the pressure inside the chamber after the emptying of the reservoir. Further tests are required to verify this theory.

During pressure measurements the valve has to be closed. The flow of IV fluid is thus halted during measurement. The clinical influence of this temporarily stop of fluid flow is not known. The settling time of the system dominates the period for which the valve needs to be closed.

The change of capacitance of the capacitor that forms the drip sensor is influenced by the type and amount of IV fluid present in the reservoir. The potential inability of the sensor to detect certain fluids (as for example purified water) and the influence of reservoir fluid volume, should be further tested.

All measurements and test were performed without a connection with the human body. The back pressure resulting from the vein was mimicked by the roller clamp. The roller clamp only restricted the outflow of fluid and it does not create the variable behaviour of the venous back pressure. Further research should be performed into the influence of this venous back pressure on the sensors and actuators functioning.

This thesis presented methods for sensing and regulation of the flow within the gravity based IV set. The functioning of the actual routine for controlling the system (chapter 5-3) is not implemented and tested. Optimization of the control routine is essential for the successful implementation of the presented sensing and regulation methods in an actual device.

Appendix A

IV selection procedure & categories

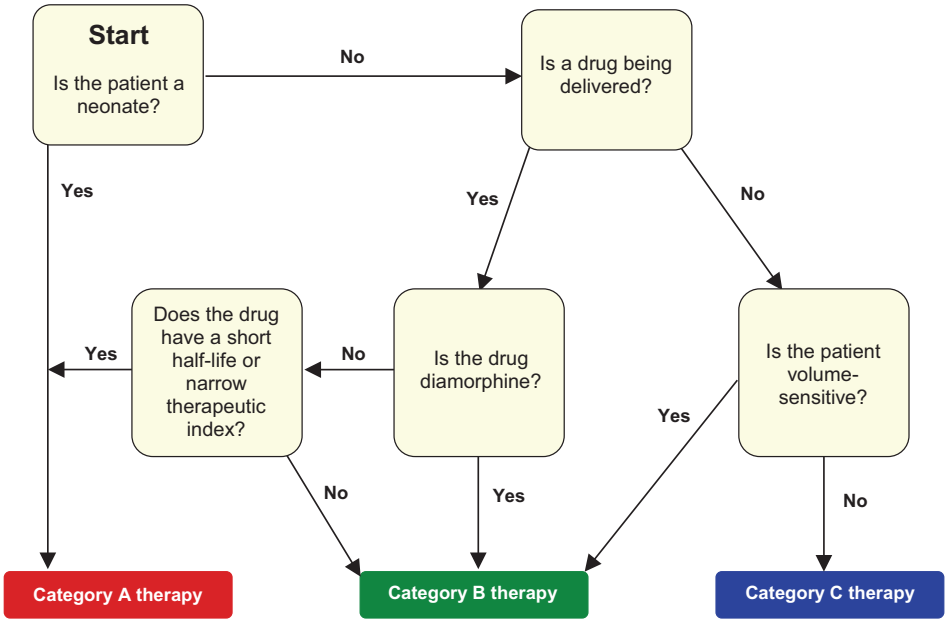

Figure A-1: Decision tree for selecting the appropriate therapy category [22]

Therapy category	Therapy description	Patient group	Critical performance parameters
A	Drugs with narrow therapeutic margin	Any	Good long-term accuracy Good short-term accuracy (see below) Rapid alarm after occlusion Small occlusion bolus Able to detect very small air embolus (volumetric pumps only) Small flow rate increments Good bolus accuracy Rapid start-up time (syringe pumps only)
	Drugs with short half-life	Any	
	Any infusion given to neonates	Neonates	
B	Drugs, other than those with a short half-life [1]	Any except neonates	Good long-term accuracy Alarm after occlusion Small occlusion bolus Able to detect small air embolus (volumetric pumps only) Small flow rate increments Bolus accuracy
	TPN Fluid maintenance Transfusions	Volume sensitive except neonates	
	Diamorphine	Any except neonates	
C	TPN Fluid maintenance Transfusions	Any except volume sensitive or neonates	Long-term accuracy Alarm after occlusion Small occlusion bolus Able to detect air embolus (volumetric pumps only) Incremental flow rates

Figure A-2: Therapy categories and performance parameters for therapy with IV pump [22]

Appendix B

Test material

B-1 MPL3115A2 breakout board

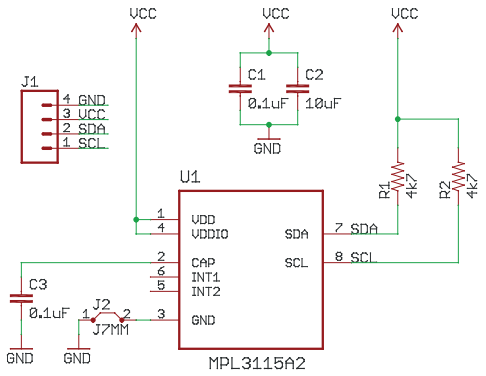

(a) breakout board circuit

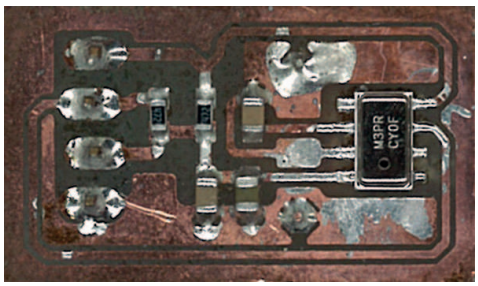

(b) breakout PCB

Figure B-1: PCB design for breakout of the MPL3115A2 sensor IC

B-2 Pressure sensing test setup

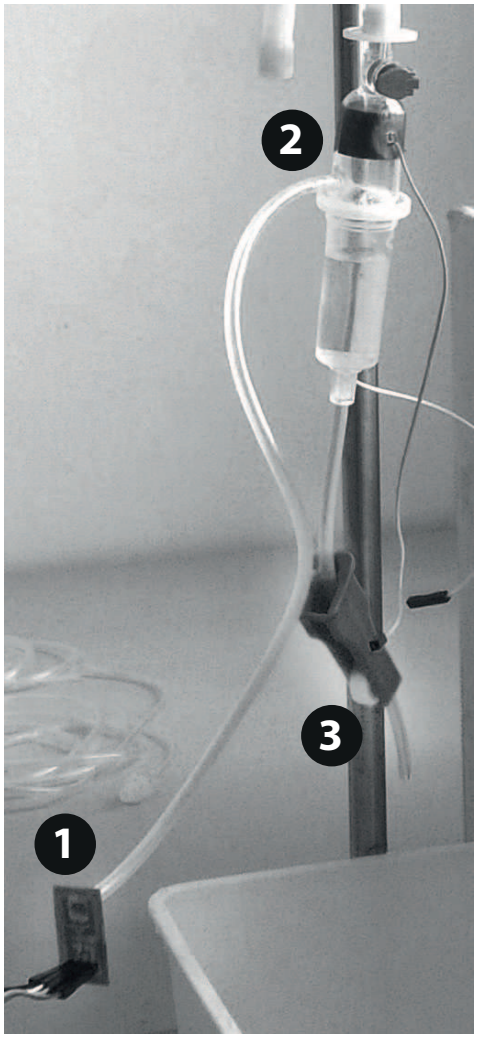

Figure B-2: Test setup for pressure measurements inside the drip chamber. Indicated are: 1. The break outboard for the MPL3115A2 pressure sensor, 2. The drip chamber and the connection of the silicone tube, 3. The roller clamp (in this picture closed, the clamping pressure is released during tests)

B-3 Sensors and valve assembly

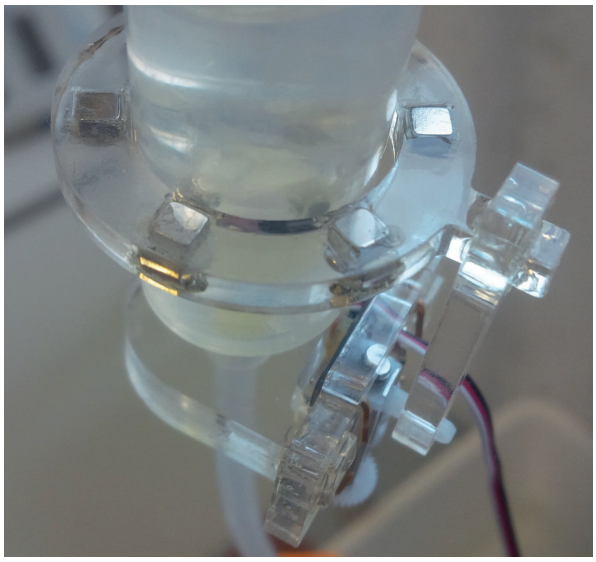

(a) View of integrated magnets in outer ring

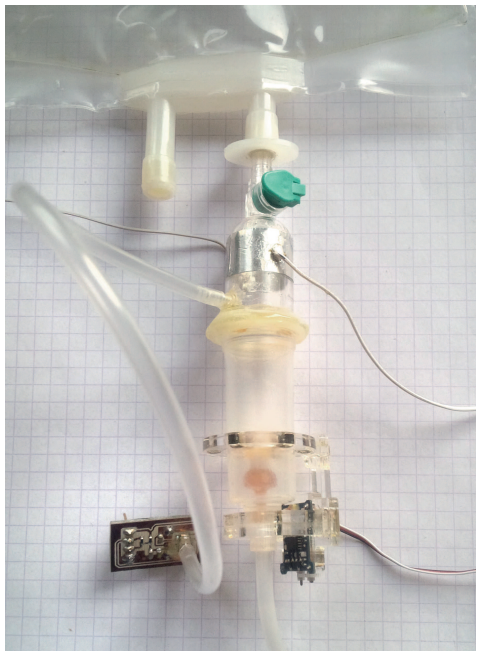

(b) Overview of test assembly

Figure B-3

Appendix C

Firmware code NHS3153

C-1 Sensor (MPL)

Code contains the specific logic for communication between NHS3153 and MPL3115A2. Initialization of I2C and pins is documented in section C-4.

```
1  /*Constant pressure measurement with NHS3153 and MPL*/
2
3  int main(void)
4  {
5    // Select data configuration register(0x13)
6    // Data ready event enabled for altitude, pressure, temperature(0x07)
7    config[0] = 0x13;
8    config[1] = 0x07;
9    Chip_I2C_MasterSend ( I2C0 , 0x60 , &config , 2); /*Transmit buffer to
         MPL*/
10
11   // Select control register(0x26)
12   // Active mode, OSR = 128 (resolution), barometer mode(0x39)
13   config[0] = 0x26;
14   config[1] = 0x39;
15   Chip_I2C_MasterSend ( I2C0 , 0x60 , &config , 2); /*Transmit buffer to
         MPL*/
16   Chip_Clock_System_BusyWait_ms (1000) ;
17
18   while (1) {
19     // Read 4 bytes of data from register(0x00) of MPL
20     // status, pres msb1, pres msb, pres lsb
21     reg[0] = 0x00;
22     Chip_I2C_MasterCmdRead( I2C0 , 0x60, &reg , &data, 4);
23
24     // Convert the data to 20-bits
25     int pres = ((data[1] * 65536) + (data[2] * 256 + (data[3] & 0xF0))) /
           16;
```

```
26
27      //Convert measurement into 3*byte for I2C transmission
28      uint8_t presl = pres;
29      uint8_t presm = (pres >> 8);
30      uint8_t presh = (pres >> 16);
31
32      //Transmission buffer for sending to Arduino
33      uint8_t buffer[3] = {0};
34      buffer[0] = presl;
35      buffer[1] = presm;
36      buffer[2] = presh;
37
38      //Transmit information to Arduino waiting for log in Matlab
39      Chip_I2C_MasterSend ( I2C0 , 0x08 , &buffer , 3);
40
41      //Delay for next measurement (2Hz)
42      Chip_Clock_System_BusyWait_ms (500);
43    }
44
45      return 0;
46  }
```

C-2 Capacitive measurement

Code contains the specific logic for measurement of capacity of capacitive drip sensor. Initialization of I2C and pins is shown in section C-4.

```
1  /*Arduino debug out I2C to serial conversion*/
2
3  int main(void)
4  {
5
6    /* C2D initialization*/
7      Chip_C2D_Init(NSS_C2D);
8      Chip_C2D_Setup(NSS_C2D, C2D_CONTINUOUS, C2D_15BITS, 2000, C2D_1000fF)
           ; //Dynamical in counts of 100, continous measurement mode
9      Chip_C2D_SetMuxAInput(NSS_C2D, C2D_INPUT_CREF1800fF);
10     Chip_C2D_SetMuxBInput(NSS_C2D, C2D_INPUT_ANA_4_5);
11     Chip_C2D_Start(NSS_C2D);
12
13     while (1) {
14     if ((Chip_C2D_ReadStatus(NSS_C2D) & C2D_STATUS_MUX_ERR) == 0) {
15       while (!(Chip_C2D_ReadStatus(NSS_C2D) & C2D_STATUS_CONVERSION_DONE)
             ) {
16         ; /* Wait until measurement completes. */
17       }
18       int cap_native = Chip_C2D_GetValue(NSS_C2D);
19
20       //Convert measurement into 4*byte for transmission
21       uint8_t capl = cap_native & 0xff ;
22       uint8_t capm = (cap_native >> 8);
```

```
23        uint8_t caph = (cap_native >> 16);
24        uint8_t pos = (stand - 9180)/10;
25
26
27        //Transmission buffer for sending to Arduino
28        uint8_t buffer[4] = {0};
29        buffer[0] = pos;
30        buffer[1] = capl;
31        buffer[2] = capm;
32        buffer[3] = caph;
33        Chip_I2C_MasterSend ( I2C0 , 0x08 , &buffer , 4); //Send
              information to arduino waiting on 0x08
34      }
35
36      }
37      Chip_C2D_DeInit(NSS_C2D);
38
39      return 0;
40  }
```

C-3 Actuation

Code contains the specific logic for PWM control of servo actuator. Initialization of I2C and pins is shown in section C-4.

```
1  /* PWM test routine min max position of servo */
2
3  int main(void)
4  {
5      Chip_TIMER16_0_Init(); /* Initialize timer of NHS for PWM */
6      Chip_TIMER_PrescaleSet(NSS_TIMER16_0, ((uint32_t)
           Chip_Clock_System_GetClockFreq() / 500000) - 1); /* scaling of
           clock freq to 500000*/
7
8    /* Enable PWM */
9    Chip_TIMER_SetMatchOutputMode(NSS_TIMER16_0, 1, TIMER_MATCH_OUTPUT_PWM)
         ;
10
11   /* MR2 -> PWM cycle time, no interrupt, no stop, reset on match */
12   Chip_TIMER_SetMatch(NSS_TIMER16_0, 2, 10000 - 1); /* 0-based MR: 0 to
         9999 (10.000 counts = 50Hz if processor speed is scaled with clock
         /500000) */
13   Chip_TIMER_MatchDisableInt(NSS_TIMER16_0, 2);
14   Chip_TIMER_StopOnMatchDisable(NSS_TIMER16_0, 2);
15   Chip_TIMER_ResetOnMatchEnable(NSS_TIMER16_0, 2);
16
17     while (1) {
18       /* MR1 -> low to high at 9000, no interrupt, no stop, no reset */
19       Chip_TIMER_SetMatch(NSS_TIMER16_0, 1, 9180 - 1); /* 9180 => 820 *
             0.002 ms = 1.64ms pulse. Closed position*/
20       Chip_TIMER_MatchDisableInt(NSS_TIMER16_0, 1);
```

```
21        Chip_TIMER_StopOnMatchDisable(NSS_TIMER16_0, 1);
22        Chip_TIMER_ResetOnMatchDisable(NSS_TIMER16_0, 1);
23
24        /* Reset TC */
25        Chip_TIMER_Reset(NSS_TIMER16_0);
26        Chip_TIMER_Enable(NSS_TIMER16_0);
27
28        /* Wait for servo to go to position */
29        Chip_Clock_System_BusyWait_ms(4000);
30
31        /* New position info */
32        Chip_TIMER_SetMatch(NSS_TIMER16_0, 1, 9640 - 1); /* 9640 max
              effective; 360 * 0.002 ms = 0.72ms pulse. Is valve open position
              */
33
34        /* Reset TC */
35        Chip_TIMER_Reset(NSS_TIMER16_0);
36        Chip_TIMER_Enable(NSS_TIMER16_0);
37
38        /* Wait for servo to go to position */
39        Chip_Clock_System_BusyWait_ms(4000);
40    }
41    return 0;
42 }
```

C-4 Sensor and actuator test routine

```
1  /*Routine for testing IV sensors and actuator*/
2
3  void I2C0_IRQHandler(void)
4  {
5      if (Chip_I2C_IsMasterActive(I2C0)) {
6          Chip_I2C_MasterStateHandler(I2C0);
7      }
8      else {
9          Chip_I2C_SlaveStateHandler(I2C0);
10     }
11 }
12
13 int main(void)
14 {
15   Board_Init();
16   Chip_Clock_System_SetClockFreq(4000000); //4MHz clock speed
17   Chip_IOCON_Init(NSS_IOCON);
18   Chip_IOCON_SetPinConfig(NSS_IOCON, { IOCON_PIO0_4, IOCON_PIO0_5 },
         IOCON_FUNC_1 | IOCON_I2CMODE_STDFAST); /* Set pin function to dig
         I2C. */
19   Chip_IOCON_SetPinConfig(NSS_IOCON, IOCON_PIO0_7, IOCON_FUNC_1); /* Set
         pin function to output (PWM). */
20
```

```
21    Chip_TIMER16_0_Init(); /* Initialize timer of NHS for PWM */
22    Chip_TIMER_PrescaleSet(NSS_TIMER16_0, ((uint32_t)
          Chip_Clock_System_GetClockFreq() / 500000) - 1); /* scaling of clock
           freq for timer to 500000*/
23
24    /* Pin 3 high for pull up of I2C, pin 3 is connected on PCB as pull up
          for I2C pin */
25    Chip_IOCON_SetPinConfig(NSS_IOCON, IOCON_PIO0_3, IOCON_FUNC_0 |
          IOCON_I2CMODE_PIO);
26    Chip_GPIO_SetPinDIROutput(NSS_GPIO, 0, 3);
27    Chip_GPIO_SetPinOutHigh(NSS_GPIO, 0, 3);
28
29    /* Enable PWM */
30    Chip_TIMER_SetMatchOutputMode(NSS_TIMER16_0, 1, TIMER_MATCH_OUTPUT_PWM)
          ;
31
32    /* MR2 -> PWM cycle time, no interrupt, no stop, reset on match */
33    Chip_TIMER_SetMatch(NSS_TIMER16_0, 2, 10000 - 1); /* 0-based MR: 0 to
          9999 (10.000 counts = 50Hz if processor speed is scaled with clock
          /500000) */
34    Chip_TIMER_MatchDisableInt(NSS_TIMER16_0, 2);
35    Chip_TIMER_StopOnMatchDisable(NSS_TIMER16_0, 2);
36    Chip_TIMER_ResetOnMatchEnable(NSS_TIMER16_0, 2);
37
38    /* I2C DeAssert */
39    Chip_SysCon_Peripheral_DeassertReset(SYSCON_PERIPHERAL_RESET_I2C0);
40
41    /* I2C Init */
42    Chip_I2C_Init(I2C0);
43    Chip_I2C_SetClockRate(I2C0, 100000); //1kHz I2C speed
44
45    /* I2C Event Handler configured to use default handler */
46    Chip_I2C_SetMasterEventHandler(I2C0, Chip_I2C_EventHandler);
47
48    /* Enable interrupt */
49    NVIC_EnableIRQ(I2C0_IRQn);
50
51    /* C2D Init */
52    Chip_IOCON_SetPinConfig(NSS_IOCON, { IOCON_ANA0_4, IOCON_ANA0_5 },
          IOCON_FUNC_1); /* Set pin 0_4 and 0_5 function to analog. */
53    Chip_C2D_Init(NSS_C2D);
54    Chip_C2D_Setup(NSS_C2D, C2D_CONTINUOUS, C2D_15BITS, 2100, C2D_800fF);
          //Dynamical in counts of 100, continous measurement mode 15 bit
          resolution, offset 800fF
55    Chip_C2D_SetMuxAInput(NSS_C2D, C2D_INPUT_CREF1800fF);
56    Chip_C2D_SetMuxBInput(NSS_C2D, C2D_INPUT_ANA_4_5);
57    Chip_C2D_Start(NSS_C2D);
58
59    /*MPL INIT */
60
61    // Select data configuration register(0x13)
62    // Data ready event enabled for altitude, pressure, temperature(0x07)
63    config[0] = 0x13;
```

```
64    config[1] = 0x07;
65    Chip_I2C_MasterSend ( I2C0 , 0x60 , &config , 2) ;
66
67    char reg[1] = {0x00};
68    char data[6] = {0};
69
70    // Select control register(0x26)
71    // Active mode, OSR = 128, barometer mode(0x39)
72    config[0] = 0x26;
73    config[1] = 0x39;
74    Chip_I2C_MasterSend ( I2C0 , 0x60 , &config , 2) ;
75    Chip_Clock_System_BusyWait_ms (1000) ;
76
77    /* MR1 -> low to high at 9000, no interrupt, no stop, no reset = CLOSE
          VALVE */
78    Chip_TIMER_SetMatch(NSS_TIMER16_0, 1, 9180 - 1); /* 9000 = 1000 * 0.02
          ms = 20ms pulse. Closed position*/
79    Chip_TIMER_MatchDisableInt(NSS_TIMER16_0, 1);
80    Chip_TIMER_StopOnMatchDisable(NSS_TIMER16_0, 1);
81    Chip_TIMER_ResetOnMatchDisable(NSS_TIMER16_0, 1);
82
83    /* Reset TC */
84    Chip_TIMER_Reset(NSS_TIMER16_0);
85    Chip_TIMER_Enable(NSS_TIMER16_0);
86
87    /* Wait for Servo to go to position and close valve */
88    Chip_Clock_System_BusyWait_ms(1000);
89
90    //ACTUAL PROGRAM
91      while (1) {
92      //PRESSURE + CAPACITANCE MEASUREMENT, NO MOVEMENT. VALVE CLOSED
93      int i = 0;
94      int stand = 9180;
95      for ( i = 0; i < 10; i++){ /* 10x 62 capacitive measurements equals
            approx 10 seconds, at same time 10x pressure measurement*/
96
97        /* Pressure measurement */
98        reg[0] = 0x00;
99        Chip_I2C_MasterCmdRead( I2C0 , 0x60, &reg , &data, 4); // Read 4
              bytes of data from register(0x00): status, pres msb1, pres msb,
              pres lsb
100
101       // Convert the data to 20-bits
102       int pres = ((data[1] * 65536) + (data[2] * 256 + (data[3] & 0xF0)))
              / 16;
103
104       /* 62 x Capacitive measurement */
105       int c2d = 0;
106       for( c2d = 0; c2d < 62; c2d = c2d + 1 ){
107         //Chip_Clock_System_BusyWait_ms(20);
108         if ((Chip_C2D_ReadStatus(NSS_C2D) & C2D_STATUS_MUX_ERR) == 0) {
109           while (!(Chip_C2D_ReadStatus(NSS_C2D) &
                  C2D_STATUS_CONVERSION_DONE)) {
```

```
110                 ; /* Wait until measurement completes. */
111               }
112             int cap_native = Chip_C2D_GetValue(NSS_C2D);
113             //Convert measurement into 7*byte for transmission by shifting
114             uint8_t capl = cap_native;
115             uint8_t capm = (cap_native >> 8);
116             uint8_t caph = (cap_native >> 16);
117             uint8_t presl = pres;
118             uint8_t presm = (pres >> 8);
119             uint8_t presh = (pres >> 16);
120             uint8_t pos = (stand - 9180)/10; //scale position data to
                    relevant part
121
122             //Transmission buffer for sending to Arduino
123             uint8_t buffer[7] = {0};
124             buffer[0] = pos;
125             buffer[1] = capl;
126             buffer[2] = capm;
127             buffer[3] = caph;
128             buffer[4] = presl;
129             buffer[5] = presm;
130             buffer[6] = presh;
131             Chip_I2C_MasterSend ( I2C0 , 0x08 , &buffer , 7); //Send
                    information to arduino waiting on 0x08
132           }
133         }
134       }
135
136       //CAPACITANCE MEASUREMENT during VALVE OPENING STEPS
137         /* for position < open */
138         for( stand = 9180; stand < 9620; stand = stand + 10 ){
139
140         /* New position info */
141         Chip_TIMER_SetMatch(NSS_TIMER16_0, 1, stand - 1);
142
143         /* Reset TC */
144         Chip_TIMER_Reset(NSS_TIMER16_0);
145         Chip_TIMER_Enable(NSS_TIMER16_0);
146
147         int c2d = 0;
148         for( c2d = 0; c2d < 62; c2d = c2d + 1 ){
149 //          Chip_Clock_System_BusyWait_ms(20);
150           if ((Chip_C2D_ReadStatus(NSS_C2D) & C2D_STATUS_MUX_ERR) == 0) {
151             while (!(Chip_C2D_ReadStatus(NSS_C2D) &
                        C2D_STATUS_CONVERSION_DONE)) {
152               ; /* Wait until measurement completes. */
153             }
154             int cap_native = Chip_C2D_GetValue(NSS_C2D);
155
156             //Convert measurement into 4*byte for transmission by shifting
157             uint8_t capl = cap_native & 0xff ;
158             uint8_t capm = (cap_native >> 8);
159             uint8_t caph = (cap_native >> 16);
```

```
160           uint8_t pos = (stand - 9180)/10; //position = total - offset
                  devided by step size
161
162
163           //Transmission buffer for sending to Arduino
164           uint8_t buffer[4] = {0};
165           buffer[0] = pos;
166           buffer[1] = capl;
167           buffer[2] = capm;
168           buffer[3] = caph;
169           Chip_I2C_MasterSend ( I2C0 , 0x08 , &buffer , 4); //Send
                  information to arduino waiting on 0x08
170         }
171       }
172     }
173
174     //CAPACITANCE MEASUREMENT, NO MOVEMENT. VALVE OPEN 2 SEC PAUSE
175       for ( i = 0; i < 2; i++){ /* 2 x 62 measurements = approx 2x1sec */
176         int c2d = 0;
177       for( c2d = 0; c2d < 62; c2d = c2d + 1 ){
178         if ((Chip_C2D_ReadStatus(NSS_C2D) & C2D_STATUS_MUX_ERR) == 0) {
179           while (!(Chip_C2D_ReadStatus(NSS_C2D) &
                      C2D_STATUS_CONVERSION_DONE)) {
180             ; /* Wait until measurement completes. */
181           }
182           int cap_native = Chip_C2D_GetValue(NSS_C2D);
183
184           //Convert measurement into 4*byte for transmission by shifting
185           uint8_t capl = cap_native & 0xff ;
186           uint8_t capm = (cap_native >> 8);
187           uint8_t caph = (cap_native >> 16);
188           uint8_t pos = (stand - 9180)/10; //position = total - offset
                  devided by step size
189
190           //Transmission buffer for sending to Arduino
191           uint8_t buffer[4] = {0};
192           buffer[0] = pos;
193           buffer[1] = capl;
194           buffer[2] = capm;
195           buffer[3] = caph;
196           Chip_I2C_MasterSend ( I2C0 , 0x08 , &buffer , 4); //Send
                  information to arduino waiting on 0x08
197         }
198       }
199     }
200
201     //CAPACITANCE MEASUREMENT, CLOSING VALVE
202     /* for position > closed */
203     for( stand = 9620; stand > 9180; stand = stand - 10 ){
204
205       /* New position info */
206       Chip_TIMER_SetMatch(NSS_TIMER16_0, 1, stand - 1);
207
```

```
208         /* Reset TC */
209         Chip_TIMER_Reset(NSS_TIMER16_0);
210         Chip_TIMER_Enable(NSS_TIMER16_0);
211 
212         int c2d = 0;
213         for( c2d = 0; c2d < 62; c2d = c2d + 1 ){
214           if ((Chip_C2D_ReadStatus(NSS_C2D) & C2D_STATUS_MUX_ERR) == 0) {
215             while (!(Chip_C2D_ReadStatus(NSS_C2D) &
                        C2D_STATUS_CONVERSION_DONE)) {
216               ; /* Wait until measurement completes. */
217             }
218             int cap_native = Chip_C2D_GetValue(NSS_C2D);
219 
220             //Convert measurement into 4*byte for transmission by shifting
221             uint8_t capl = cap_native & 0xff ;
222             uint8_t capm = (cap_native >> 8);
223             uint8_t caph = (cap_native >> 16);
224             uint8_t pos = (stand - 9180)/10; //position = total - offset
                        devided by step size
225 
226             //Transmission buffer for sending to Arduino
227             uint8_t buffer[4] = {0};
228             buffer[0] = pos;
229             buffer[1] = capl;
230             buffer[2] = capm;
231             buffer[3] = caph;
232             Chip_I2C_MasterSend ( I2C0 , 0x08 , &buffer , 4); //Send
                        information to arduino waiting on 0x08
233           }
234         }
235       }
236     }
237 
238       Chip_C2D_DeInit(NSS_C2D);
239       return 0;
240 }
```

Appendix D

Arduino code

D-1 Data conversion debug out

```
1  /*Arduino debug out I2C to serial conversion*/
2
3  void setup() {
4    Wire.begin(8);                // join i2c bus as slave with address 0
         x08
5    Wire.onReceive(receiveEvent); // register event
6    Serial.begin(9600);           // start serial for output
7  }
8
9  void loop() {
10   delay(100);
11 }
12
13 // function that executes whenever data is received from master
14 // this function is registered as an event, see setup()
15 void receiveEvent(int howMany) {
16   byte data[7];
17   if (Wire.available() == 4)  // only if 4 bytes info without pressure
18   {
19     data[0] = Wire.read();
20     data[1] = Wire.read();
21     data[2] = Wire.read();
22     data[3] = Wire.read();
23
24     /*assemble received bytes by shifting*/
25     uint32_t capacitance;
26     capacitance = data[3];
27     capacitance = (capacitance << 8)  | data[2];
28     capacitance = (capacitance << 8)  | data[1];
29
```

```
30      int stand = data[0];     // stand = pwm position
31
32    //Outpute to serial received assembled info
33      Serial.print(stand);
34      Serial.print(" ");
35      Serial.print(capacitance);
36      Serial.print(" ");
37      Serial.println("nan");
38    }
39
40    if (Wire.available() == 7)  // 7 bytes is with pressure info
41    {
42      data[0] = Wire.read();
43      data[1] = Wire.read();
44      data[2] = Wire.read();
45      data[3] = Wire.read();
46      data[4] = Wire.read();
47      data[5] = Wire.read();
48      data[6] = Wire.read();
49
50      int stand = data[0];     // stand = pwm position
51
52      /*assemble received bytes by shifting*/
53      uint32_t capacitance;
54      capacitance = data[3];
55      capacitance = (capacitance << 8)  | data[2];
56      capacitance = (capacitance << 8)  | data[1];
57
58      uint32_t pres;
59      pres = data[6];
60      pres = (pres << 8)  | data[5];
61      pres = (pres << 8)  | data[4];
62      uint32_t pressure = pres/4.0;
63
64    //Outpute to serial received assembled info
65      Serial.print(stand);
66      Serial.print(" ");
67      Serial.print(capacitance);
68      Serial.print(" ");
69      Serial.println(pressure);
70    }
71  }
```

Appendix E

Matlab code

E-1 Peak detection, filtering and plot of data

```
%IV data filtering and peakfinder

clear
clc

%Initial data loading
load 161121.mat
data = data;
cap = data(2,1:end)';
pos = data(1,1:end)';
pos = (pos/32)*100;

%Three subplots
ax1 = subplot(3,1,1);
plot (time,pos);

ax2 = subplot(3,1,2);
smoothcap = sgolayfilt(cap,3,21); %Savitzky-Golay filter on raw data
[pks, locs] = findpeaks(-smoothcap,time,'MinPeakProminence',70); %detect
    negative peaks
plot(time,smoothcap,locs, -pks,'ko','MarkerSize',5)
peakInterval = diff(locs);
freq = 1./peakInterval;

ax3 = subplot(3,1,3);
plot (locs(2:end), freq);

%Formatting of plots
axis([ax1,ax2,ax3], [0 1050 -inf inf]);
ylabel(ax1, 'PWM (0-100%)');
```

```
30 xlabel(ax1, 'time (s)');
31 ylabel(ax2, 'capacitance raw');
32 xlabel(ax2, 'time (s)');
33 ylabel(ax3, 'drip freq (Hz)');
34 xlabel(ax3, 'time (s)');
35
36 grid(ax1, 'on');
37 grid(ax2, 'on');
38 grid(ax3, 'on');
```

Bibliography

[1] D. Millam, "The history of intravenous therapy," *J Intraven Nurs*, vol. 19, no. 1, pp. 5–14, 1996.

[2] L. Baranowski, "Presidential address: take ownership," *J Intraven Nurs*, vol. 18, no. 4, pp. 162–4, 1995.

[3] M. Husch, C. Sullivan, D. Rooney, C. Barnard, M. Fotis, J. Clarke, and G. Noskin, "Insights from the sharp end of intravenous medication errors: implications for infusion pump technology," *Qual Saf Health Care*, vol. 14, no. 2, pp. 80–6, 2005.

[4] IEC, "Particular requirements for the basic safety and essential performance of infusion pumps and controllers," IEC 60601-2-24-2010, International Electrotechnical Commission, 2010.

[5] J. D. Bronzino, *Parenteral Infusion Devices - The Biomedical Engineering Handbook*. CRC Press, 2000.

[6] ISO, "Infusion equipment for medical use - Part 4: Infusion sets for single use, gravity feed," ISO 8536-4:2010, International Organization for Standardization, Geneva, Switzerland, 2010.

[7] F. C. Flack and T. D. Whyte, "Behaviour of standard gravity-fed administration sets used for intravenous infusion," *Br Med J*, vol. 3, no. 5928, pp. 439–43, 1974.

[8] J. H. Philip, "Model for the physics and physiology of fluid administration," *J Clin Monit*, vol. 5, no. 2, pp. 123–34, 1989.

[9] D. La Cour, "Drop size in intravenous infusion," *Acta Anaesthesiol Scand Suppl*, vol. 24, pp. 35–41, 1966.

[10] "Adelberg v-clamp profile." http://www.adelberglaboratories.com/compare.html. Accessed: December 2016.

[11] M. Disselkoen, "A literature review on methods of flow-rate measurement in iv therapy," report, TU Delft, Delft, the Netherlands, 2016.

[12] G. Schnell, "Measurement of flow in infusion systems," *Med Biol Eng Comput*, vol. 35, no. 6, pp. 737–41, 1997.

[13] W. Zhang, W. Zhou, Z. Liu, W. Zhang, and Z. Liu, "Drips detection sensor of cylindrical surface capacitor," in *Electrical and Control Engineering (ICECE), International Conference on*, pp. 653–656, 2011.

[14] C. Fuh-Gwo, W. Jen-Ya, C. Shian, T. Sheng-Chung, and C. Kuo-Yi, "A hang-and-play intravenous infusion monitoring system," in *Applied Computing and Information Technology/2nd International Conference on Computational Science and Intelligence (ACIT-CSI), 3rd International Conference on*, pp. 278–281.

[15] A. Cataldo, G. Cannazza, N. Giaquinto, A. Trotta, and G. Andria, "Development of a remote system for real-time control of intravenous drip infusions," in *Medical Measurements and Applications Proceedings (MeMeA), IEEE International Workshop on*, pp. 234–237, 2011.

[16] A. Cataldo, G. Cannazza, N. Giaquinto, A. Trotta, and G. Andria, "Microwave tdr for real-time control of intravenous drip infusions," *Instrumentation and Measurement, IEEE Transactions on*, vol. 61, no. 7, pp. 1866–1873, 2012.

[17] A. Cataldo, G. Cannazza, E. De Benedetto, N. Giaquinto, and A. Trotta, "Reproducibility analysis of a tdr-based monitoring system for intravenous drip infusions: Validation of a novel method for flow-rate measurement in iv infusion," in *Medical Measurements and Applications Proceedings (MeMeA), IEEE International Symposium on*, pp. 1–5, 2012.

[18] NXP Semiconductors, *MPL3115A2 - I2C precision pressure sensor with altimetry*, 9 2016. Rev. 5.1.

[19] NXP Semiconductors, *MP3V5004G - Differential and Gauge, Integrated Pressure Sensor*, 6 2010. Rev. 2.

[20] O. Tremblay and L. Dessaint, "Experimental validation of a battery dynamic model for ev applications," *World Electric Vehicle Journal*, vol. 3, pp. 289–298, 2009.

[21] "Hobbyking - hk3d-1.7r." https://hobbyking.com/. Accessed: December 2016.

[22] MHRA, "Infusion systems - guidance for healthcare professions on using and managing infusion systems," report, Medicines and Healthcare products Regulatory Agency, 2013.

Glossary

List of Acronyms

IV	Intravenous
TDR	Time-domain reflectometry
C2D	capacitance to digital
SNR	Signal to Noise Ratio
PCB	Printed circuit board
IC	Integrated Circuit
KVO	keep vein open
PWM	pulse width modulated
IC	Integrated Circuit
SDK	Software Development Kit